

Supporting Information

Motualevic Acids A-F, Antimicrobial Acids from the Sponge *Siliquariaspongia* sp.

Jessica L. Keffer, Alberto Plaza, Carole A. Bewley*

*Laboratory of Bioorganic Chemistry, National Institute of Diabetes and Digestive and Kidney Diseases, National
Institutes of Health, Bethesda, MD, 20892*

caroleb@mail.nih.gov

Table of Contents

Table of Contents	1-2
Experimental Section	3-4
Tables S1-S6. Tabulated NMR data for 1-7	5-7
Physical Data	8
Figure S1. ¹ H NMR spectrum of 1 in CD ₃ OD	9
Figure S2. ¹³ C NMR spectrum of 1 in CD ₃ OD	10
Figure S3. HSQC spectrum of 1 in CD ₃ OD	11
Figure S4. HMBC spectrum of 1 in CD ₃ OD	12
Figure S5. TOCSY spectrum of 1 in CD ₃ OD	13
Figure S6. COSY spectrum of 1 in CD ₃ OD	14
Figure S7. ¹ H NMR spectrum of 2 in CD ₃ OD	15
Figure S8. HSQC spectrum of 2 in CD ₃ OD	16
Figure S9. HMBC spectrum of 2 in CD ₃ OD	17
Figure S10. TOCSY spectrum of 2 in CD ₃ OD	18
Figure S11. COSY spectrum of 2 in CD ₃ OD	19
Figure S12. ¹ H NMR spectrum of 3 in CD ₃ OD	20

Figure S13. ^1H NMR spectrum of 3 in CDCl_3	21
Figure S14. ^{13}C NMR spectrum of 3 in CDCl_3	22
Figure S15. HSQC spectrum of 3 in CD_3OD	23
Figure S16. HMBC spectrum of 3 in CD_3OD	24
Figure S17. COSY spectrum of 3 in CDCl_3	25
Figure S18. ^1H NMR spectrum of 4 in CD_3OD	26
Figure S19. HSQC spectrum of 4 in CD_3OD	27
Figure S20. HMBC spectrum of 4 in CD_3OD	28
Figure S21. ^1H NMR spectrum of 5 in CDCl_3	29
Figure S22. ^{13}C NMR spectrum of 5 in CDCl_3	30
Figure S23. HSQC spectrum of 5 in CDCl_3	31
Figure S24. HMBC spectrum of 5 in CDCl_3	32
Figure S25. COSY spectrum of 5 in CDCl_3	33
Figure S26. ^1H NMR spectrum of 6 in CDCl_3	34
Figure S27. ^{13}C NMR spectrum of 6 in CDCl_3	35
Figure S28. HSQC spectrum of 6 in CDCl_3	36
Figure S29. HMBC spectrum of 6 in CDCl_3	37
Figure S30. COSY spectrum of 6 in CDCl_3	38
Figure S31. ^1H NMR spectrum of 7 in CDCl_3	39
Figure S32. HSQC spectrum of 7 in CDCl_3	40
Figure S33. HMBC spectrum of 7 in CDCl_3	41
Figure S34. COSY spectrum of 7 in CDCl_3	42
Figure S35. Chiral HPLC chromatogram of 6	43

Experimental Section

General Experimental Procedures. Optical rotations were measured with a Jasco P-2000 polarimeter and UV spectra were recorded on an Agilent 8453 spectrophotometer. NMR spectra were recorded on a Bruker Avance DRX-500 spectrometer equipped with a cryogenically cooled probe and *z*-shielded gradients. DQFCOSY, 2D-HOHAHA, HSQC, HMBC, and ROESY experiments were recorded using standard pulse programs. Delays in HSQC and HMBC experiments were set for $^1J_{C-H} = 145$ Hz and $^{2,3}J_{C-H} = 8$ and 5 Hz, respectively. The accurate mass electrospray ionization (ESI) mass spectra were measured on a Waters LCT Premier time-of-flight (TOF) mass spectrometer. The instrument was operated in *W*-mode at a nominal resolution of 10,000. The electrospray capillary voltage was set at 2KV and the sample cone voltage at 60 volts. The desolvation temperature was set to 275 °C and nitrogen was used as the desolvation gas with a flow rate of 300 L/hr. Accurate masses were obtained using the internal reference standard method.

Sponge material. Samples of *Siliquariaspongia* sp. (deLaubenfels, 1954) (lithistid Demospongiae: family Theonellidae) were collected in Fiji at a depth of 40 m in 2000. A voucher specimen has been deposited at the Natural History Museum, London, United Kingdom. Samples were frozen immediately after collection, and shipped frozen to Frederick, MD, where they were freeze-dried and extracted first with H₂O and subsequently with MeOH:CH₂Cl₂ (1:1) to give crude aqueous and organic extracts, respectively.

Extraction and Isolation. Isolation and purification were guided by antibacterial activity at each step. The aqueous extract (6 g) was partitioned between *n*-BuOH-H₂O (1:1) and the *n*-BuOH removed *in vacuo* from the active fraction to give 0.6 g of material. The organic extract (2 g) was partitioned sequentially with hexanes:MeOH:H₂O (10:9:1) and CHCl₃:MeOH:H₂O (10:6:4), and the solvent removed *in vacuo* to give 0.4 g of a dried chloroform extract. Less than 10 mg were obtained from the other inactive layers, neither of which were analyzed further. Both extracts were fractionated on a Sephadex LH-20 column (50 x 2.5 cm) using MeOH:H₂O (3:1) as the mobile phase. Fractions containing the fatty acids were combined and the solvent removed *in vacuo* to give 73 mg from the chloroform extract and 108 mg from the *n*-butanol extract. These samples were chromatographed by reverse-phase HPLC (Jupiter Fusion, 250 x 10 mm, 4 μm, detection at 220 and 254 nm) eluting with a linear gradient of 65–85 % MeOH in 0.05% TFA in 42 minutes to afford motualevic acids A (**1**, 18.6 mg, $t_R=45.2$ min), B (**2**, 1.5 mg, $t_R=46.2$ min), C (**3**, 0.7 mg, $t_R=42.7$ min), D (**4**, 1.3 mg, $t_R=47.8$ min),

E (**5**, 1.1 mg, t_R =53.7 min), and F (**6**, 27.2 mg, t_R =48.9 min), and (4*E*)-*R*-antazirine (**7**, 0.6 mg, t_R =53.9 min).

Chiral HPLC Analysis: Chiral HPLC analysis was carried out using a YMC Chiral NEA column, eluting with 0.01% TFA in 70:30 hexanes:*i*-PrOH at a flowrate of 0.5 mL/min, and peaks integrated to give percent enantiomeric excess.

Biological assays. Compounds **1-7** were tested for antimicrobial activity against *Staphylococcus aureus* (ATCC 25923), and MRSA (ATCC BAA-41) using a modified disk diffusion assay. Agar plates seeded with suspensions of bacteria were prepared by adding 500 μ L of a 24 h culture of bacteria to 100 mL of autoclaved Mueller Hinton II agar and cooled to 55 °C. Seeded liquid agar (10 mL) was transferred immediately to square Petri dishes and allowed to cool for 1 h. Control drugs used for each microorganism included kanamycin (50 μ g) for *S. aureus*, and nitrofurantoin (25 μ g) for MRSA. Following incubation at 37°C for 18 h, zones of inhibition were measured. MIC₅₀ values for compounds **1**, **3**, and **6** were determined using a microbroth dilution assay outlined in the Clinical and Laboratory Standards Institute methods for susceptibility tests for bacteria that grow aerobically.

Cytotoxicity assays using vertebrate kidney and colon tumor cell lines (BSC-1 and HCT-116, respectively) were carried out using an MTT cell proliferation assay kit (American Type Culture Collection) according to the instructions provided. Briefly, cells were seeded in 96-well tissue culture plates at a density of 2×10^4 cells/well in 50 μ L of Eagle's Essential Minimal Media (E-MEM) and allowed to adhere for 18 hr at 37 °C, 5% CO₂. Attached cells were incubated with inhibitors for 24 hr, after which the media was diluted 3-fold with fresh growth media. Following an additional 48 h incubation period, cell viability was assessed upon treatment with MTT (A₅₇₀, Molecular Devices 96-well absorbance plate reader). Motualevic acid A (**1**) was non-cytotoxic to both cell lines at concentrations as high as 100 μ g/mL and azirine **6** exhibited IC₅₀ values of 20 and 15 μ g/mL toward BSC-1 and HCT-116 cells lines, respectively.

Tabulated NMR data for 1-7

Table S1. NMR spectroscopic data for **1** in DMSO-*d*₆

	$\delta_{\text{C}}^{\text{a}}$	$\delta_{\text{H}}^{\text{b}}$ (<i>J</i> in Hz)
1	166.8	
2	124.5	5.99 d (15.6)
3	128.3	7.71 dt (15.6, 6.5)
4	30.9	2.10 dd (6.5, 13.6)
5	27.3	1.38 m
6	30.3	1.35
7	30.3	1.35
8	30.3	1.35
9	30.3	1.35
10	30.3	1.35
11	28.5	1.25 m
12	32.2	2.03 dd (14.5, 7.2)
13	139.0	6.59 t (7.2)
14	89.2	
1'	172.7	
2'	42.5	3.53 s
NH		7.65 s

^aRecorded at 125 MHz, referenced to residual DMSO-*d*₆ at δ 39.51 ppm. ^bRecorded at 500 MHz, referenced to residual DMSO-*d*₆ at δ 2.50 ppm.

Table S2. NMR spectroscopic data for **2** in CD₃OD

	$\delta_{\text{C}}^{\text{a}}$	$\delta_{\text{H}}^{\text{b}}$ (<i>J</i> in Hz)
1	169.0	
2	122.9	5.88 d (11.6)
3	146.5	6.05 dt (11.6, 7.5)
4	29.6	2.65 dd (7.5, 14.4)
5	30.2	1.45 m
6	30.3	1.34
7	30.3	1.34
8	30.3	1.34
9	30.3	1.34
10	30.3	1.34
11	28.7	1.46 m
12	33.8	2.13 dd (14.6, 7.3)
13	140.1	6.50 t (7.3)
14	89.1	
1'	175.1	
2'	43.2	3.86 s
NH		

^aRecorded at 125 MHz, referenced to residual CD₃OD at δ 49.15 ppm. ^bRecorded at 500 MHz, referenced to residual CD₃OD at δ 3.33 ppm.

Table S3. NMR spectroscopic data for **3** in CDCl₃

	$\delta_{\text{C}}^{\text{a}}$	$\delta_{\text{H}}^{\text{b}}$ (<i>J</i> in Hz)
1	166.9	
2	122.1	5.82 d (15.2)
3	146.9	6.85 dt (15.2, 7.0)
4	32.1	2.18 dd (7.0, 14.0)
5	27.9	1.42 m
6	28.9	1.26
7	28.9	1.26
8	28.9	1.26
9	28.9	1.26
10	28.9	1.26
11	27.7	1.38 m
12	33.0	2.06 dd (14.7, 7.4)
13	138.8	6.36 t (7.4)
14	88.4	
1'	171.8	
2'	43.2	4.02 s
NH		6.17 s
NH ₂		6.08 s

^aRecorded at 125 MHz, referenced to residual CDCl₃ at δ 77.23 ppm. ^bRecorded at 500 MHz, referenced to residual CDCl₃ at δ 7.24 ppm.

Table S4. NMR spectroscopic data for **4** in CD₃OD

	$\delta_{\text{C}}^{\text{a}}$	$\delta_{\text{H}}^{\text{b}}$ (<i>J</i> in Hz)
1	168.4	
2	124.1	6.04 d (15.3)
3	145.8	6.83 dt (15.3, 7.3)
4	32.6	2.24 dd (7.3, 14.4)
5	29.2	1.50 m
6	30.0	1.35
7	30.0	1.35
8	30.0	1.35
9	30.0	1.35
10	30.0	1.35
11	28.1	1.46 m
12	33.9	2.13 dd (7.3, 14.6)
13	140.0	6.50 t (7.3)
14	88.6	
1'	170.2	
2'	41.6	4.14 s
NMe-1	36.4	3.08 s
NMe-2	35.2	2.98 s

^aRecorded at 125 MHz, referenced to residual CD₃OD at δ 49.15 ppm. ^bRecorded at 500 MHz, referenced to residual CD₃OD at δ 3.33 ppm.

Table S5. NMR spectroscopic data for **5** in CDCl₃

	δ_C^a	δ_H (J in Hz) ^b
1	169.0	
2	119.9	5.82 d (15.6)
3	152.9	7.06 dt (15.6, 6.95)
4	32.6	2.22 dd (6.95, 14.5)
5	28.0	1.45 m
6	29.4	1.27 ^c
7	29.4	1.27 ^c
8	29.4	1.27 ^c
9	29.4	1.27 ^c
10	29.4	1.27 ^c
11	27.9	1.40 m
12	33.3	2.07 dd (14.6, 7.3)
13	139.0	6.37 t (7.3)
14	88.7	

^aRecorded at 125 MHz, referenced to residual CDCl₃ at δ 77.23 ppm. ^bRecorded at 500 MHz, referenced to residual CDCl₃ at δ 7.24 ppm.

Table S6. NMR spectroscopic data for **6** and **7** in CDCl₃

carbon	δ_C^a		δ_H (J in Hz) ^b		HMBC ^c
	6^d	7^e	6^f	7^g	
1	177.6	172.6			
2	28.0	28.3	2.55 s	2.56 s	C1, C3 C4
3	156.1	156.9			
4	112.7	113.1	6.53 d (15.6)	6.53 d (15.6)	C3, C5, C6, C7
5	156.6	155.9	6.72 dt (15.6, 6.85)	6.68 dt (15.6, 6.9)	C3, C4, C6, C7
6	33.5	33.4	2.36 dd (6.85, 14.4)	2.35 dd (6.9, 14.1)	C4, C5, C7, C8
7	28.2	28.3	1.50 m	1.50 m	C5, C6, C8
8	29.2	29.4	1.27	1.27	
9	29.4	29.4	1.27	1.27	
10	29.4	29.4	1.27	1.27	
11	29.4	29.4	1.27	1.27	
12	29.4	29.4	1.27	1.27	
13	28.2	28.2	1.39 m	1.40 m	C12, C14, C15
14	33.2	33.1	2.07 dd (14.6, 7.2)	2.07 dd (14.6, 7.2)	C12, C13, C15, C16
15	139.1	139.1	6.36 t (7.2)	6.37 t (7.2)	C13, C14, C16
16	88.7	88.7			
O-Me		52.5		3.71 s	

^aRecorded at 125 MHz, referenced to residual CDCl₃ at δ 77.23 ppm. ^bReferenced to residual CDCl₃ at δ 7.24 ppm. ^cProton showing HMBC correlation to indicated carbon. ^d δ_C values for motualevic acid **F** (**6**). ^e δ_C values for (4*E*)-*R*-antazirine (**7**). ^f δ_H values for motualevic acid **F** (**6**); ^g δ_H values for (4*E*)-*R*-antazirine (**7**).

Physical Data

Motualevic acid A (1): colorless, amorphous solid; UV (MeOH) λ_{\max} (log ϵ) 204 (4.89), 226 (4.08), 250 (3.69) nm; IR (film) ν 2921, 2849, 1698, 1669, 1601, 1551, 1233 cm^{-1} ; ^1H and ^{13}C NMR data, see Table 1 (CD_3OD), and S1 ($\text{DMSO}-d_6$); HR-ESI-MS m/z 436.0126 $[\text{M}-\text{H}]^+$ (calculated for $\text{C}_{16}\text{H}_{24}\text{Br}_2\text{NO}_3$, 436.0123).

Motualevic acid B (2): colorless, amorphous solid; UV (MeOH) λ_{\max} (log ϵ) 204 (4.95), 226 (4.12), 250 (3.72) nm; IR (film) ν 2923, 2844, 1699, 1664, 1603, 1553, 1230 cm^{-1} ; ^1H and ^{13}C NMR data, CD_3OD , see Table S2; HR-ESI-MS m/z 438.0275 $[\text{M}+\text{H}]^+$ (calculated for $\text{C}_{16}\text{H}_{26}\text{Br}_2\text{NO}_3$, 438.0276).

Motualevic acid C (3): colorless, amorphous solid; UV (MeOH) λ_{\max} (log ϵ) 206 (4.90), 226 (3.98), 256 (4.05) nm; IR (film) ν 2940, 2825, 1680, 1664, 1600, 1451, 1207 cm^{-1} ; ^1H and ^{13}C NMR data (CDCl_3), see Table S3; HR-ESI-MS m/z 437.0446 $[\text{M}+\text{H}]^+$ (calculated for $\text{C}_{16}\text{H}_{27}\text{Br}_2\text{N}_2\text{O}_2$, 437.0439).

Motualevic acid D (4): colorless, amorphous solid; UV (MeOH) λ_{\max} (log ϵ) 208 (4.93), 226 (4.01), 256 (4.09) nm; IR (film) ν 2945, 2820, 1678, 1674, 1620, 1448, 1200 cm^{-1} ; ^1H and ^{13}C NMR data (CD_3OD), see Table S4; HR-ESI-MS m/z 465.0746 $[\text{M}+\text{H}]^+$ (calculated for $\text{C}_{18}\text{H}_{31}\text{Br}_2\text{N}_2\text{O}_2$, 465.0752).

Motualevic acid E (5): colorless, amorphous solid; UV (MeOH) λ_{\max} (log ϵ) 210 (3.37), 228 (3.20), 254 (3.10) nm; IR (film) ν 2900, 2854, 1650, 1600, 1201 cm^{-1} ; ^1H and ^{13}C NMR data (CDCl_3), see Table S5; HR-ESI-MS m/z 378.9908 $[\text{M}-\text{H}]^+$, (calculated for $\text{C}_{14}\text{H}_{21}\text{Br}_2\text{O}_2$, 378.9908).

Motualevic acid F (6): pale yellow, amorphous solid; $[\alpha]_D$ -74.0 (c 0.1, MeOH); UV (MeOH) λ_{\max} (log ϵ) 204 (4.69), 230 (4.11), 250 (3.80) nm; IR (film) ν 2925, 2853, 1770, 1700, 1458, 1429, 1230, 1203, 1141 cm^{-1} ; ^1H and ^{13}C NMR data (CDCl_3), see Table S6; HR-ESI-MS m/z 418.0009 $[\text{M}-\text{H}]^+$ (calculated for $\text{C}_{16}\text{H}_{22}\text{Br}_2\text{NO}_2$, 418.0017).

(4E)-R-antazirine (7): pale yellow, amorphous solid; $[\alpha]_D$ -7.3 (c 0.1, MeOH); ^1H and ^{13}C NMR data (CDCl_3), see Table S6; HR-ESI-MS m/z 434.0310 $[\text{M}+\text{H}]^+$ (calculated for $\text{C}_{17}\text{H}_{26}\text{Br}_2\text{NO}_2$, 434.0330).

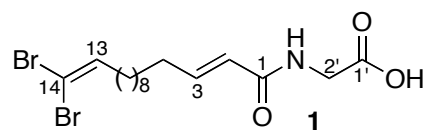
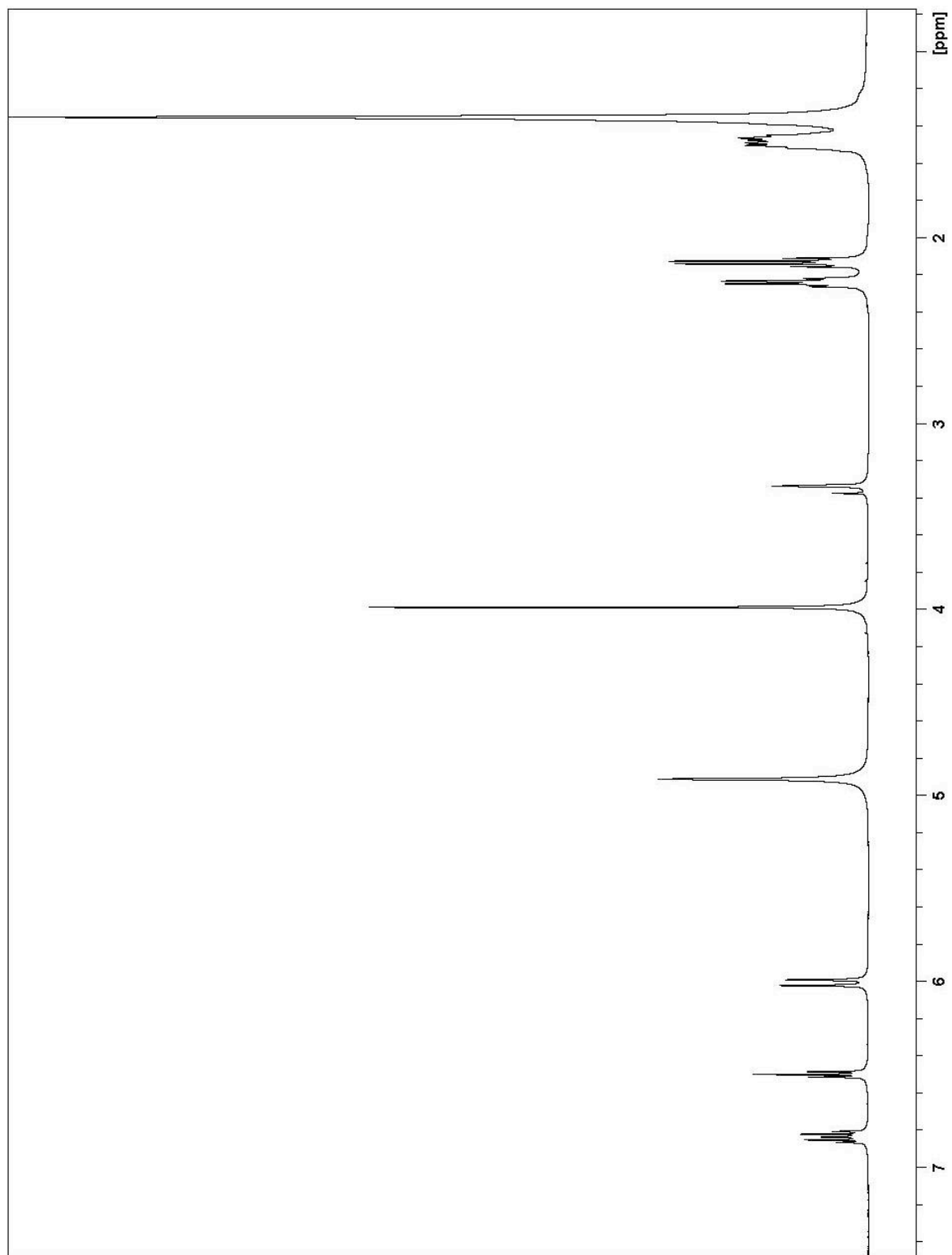


Figure S1. ^1H NMR spectrum of motualevic acid A (**1**) in CD_3OD .

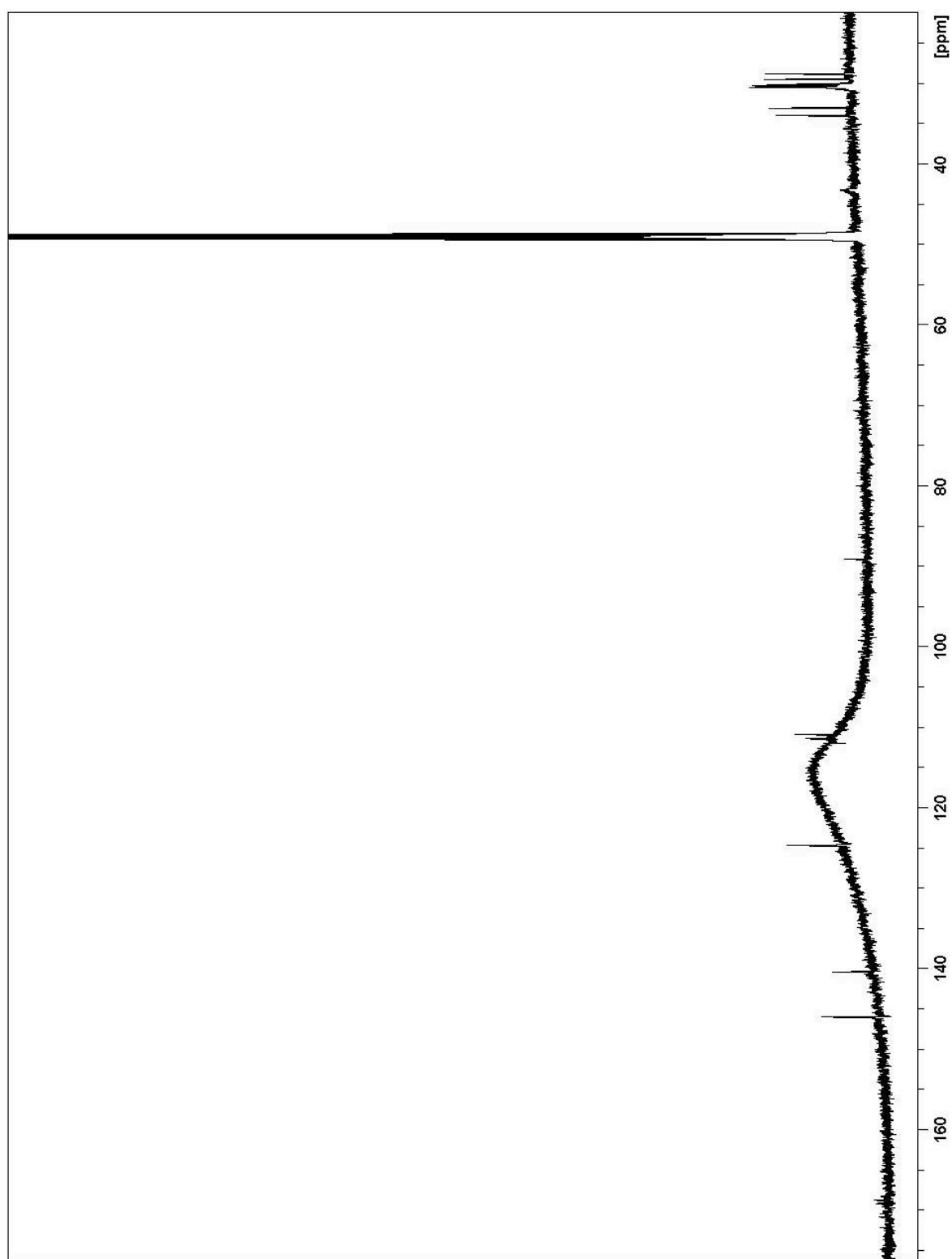


Figure S2. ^{13}C NMR spectrum of motualevic acid A (**1**) in CD_3OD .

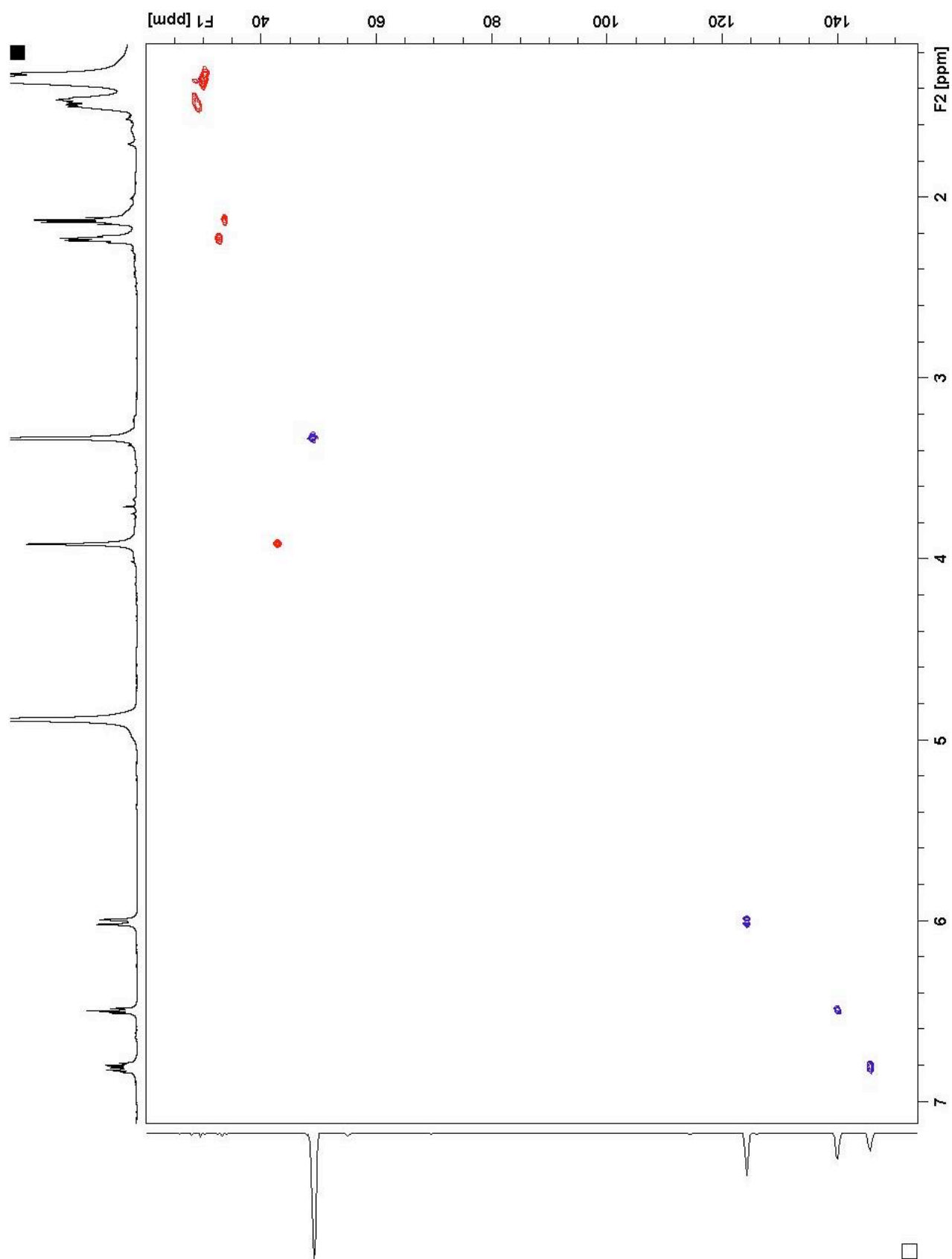


Figure S3. HSQC spectrum of motualevic acid A (1) in CD₃OD.

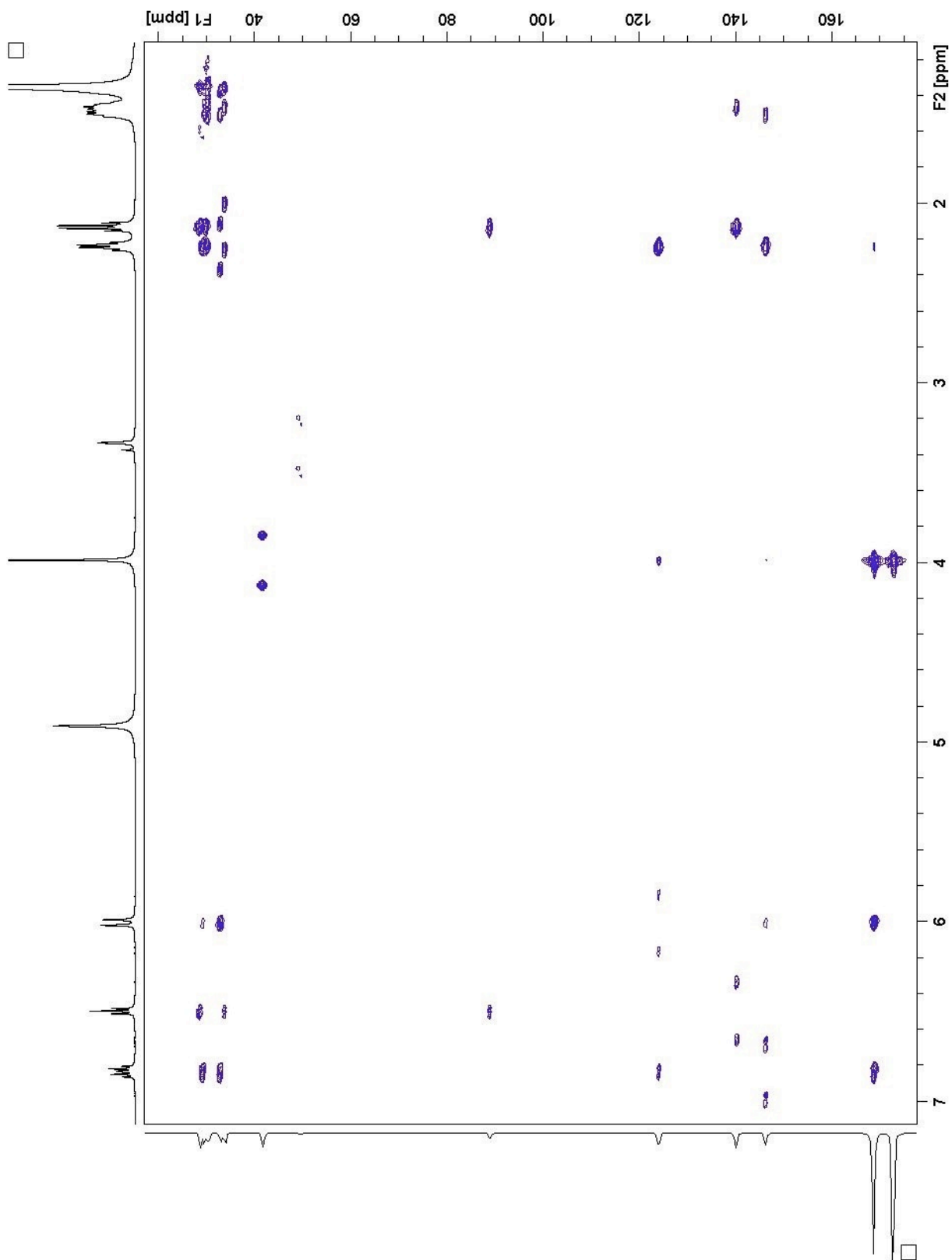


Figure S4. HMBC spectrum of motualevic acid A (1) in CD_3OD .

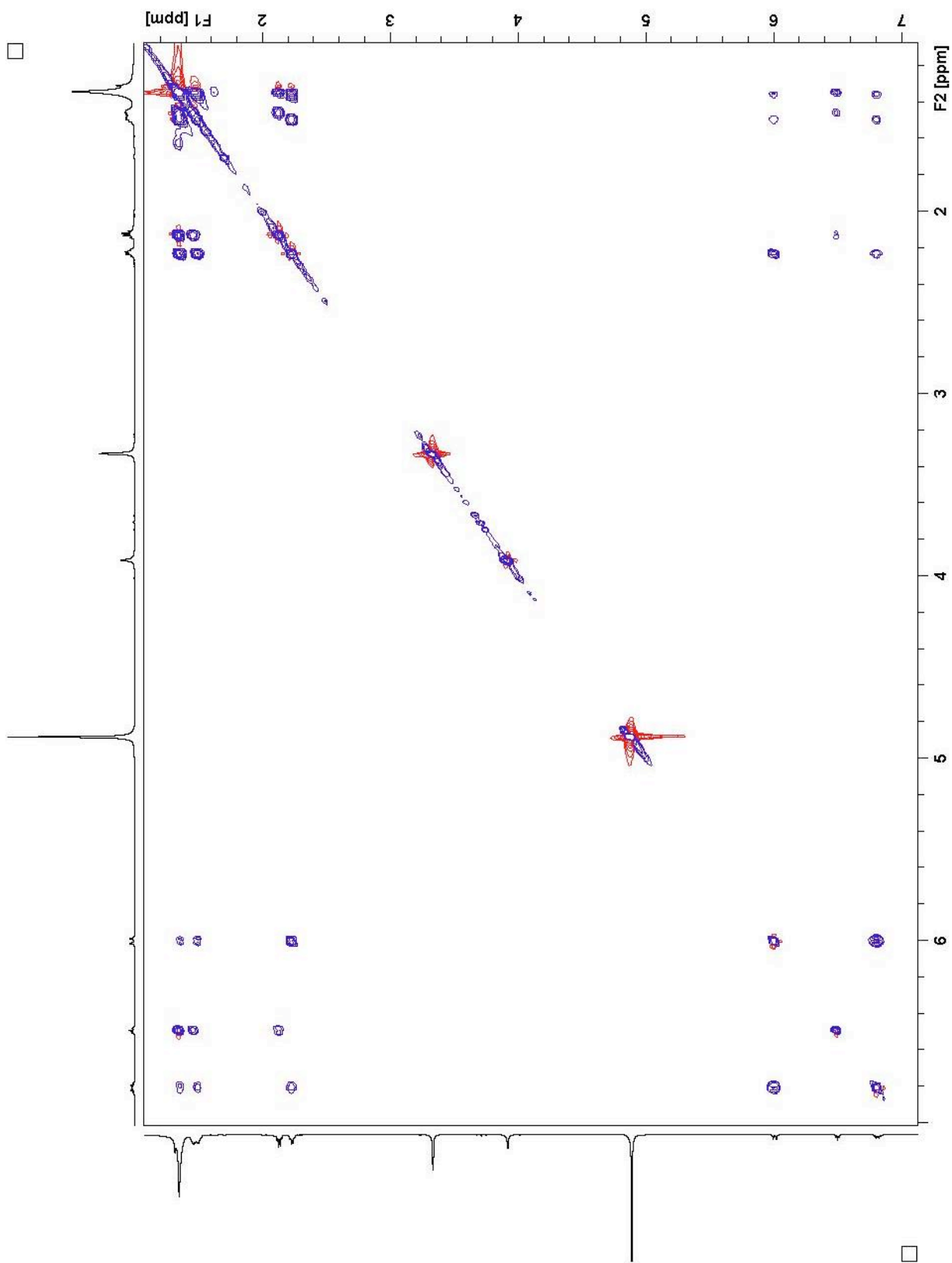


Figure S5. TOCSY spectrum of motualevic acid A (**1**) in CD₃OD.

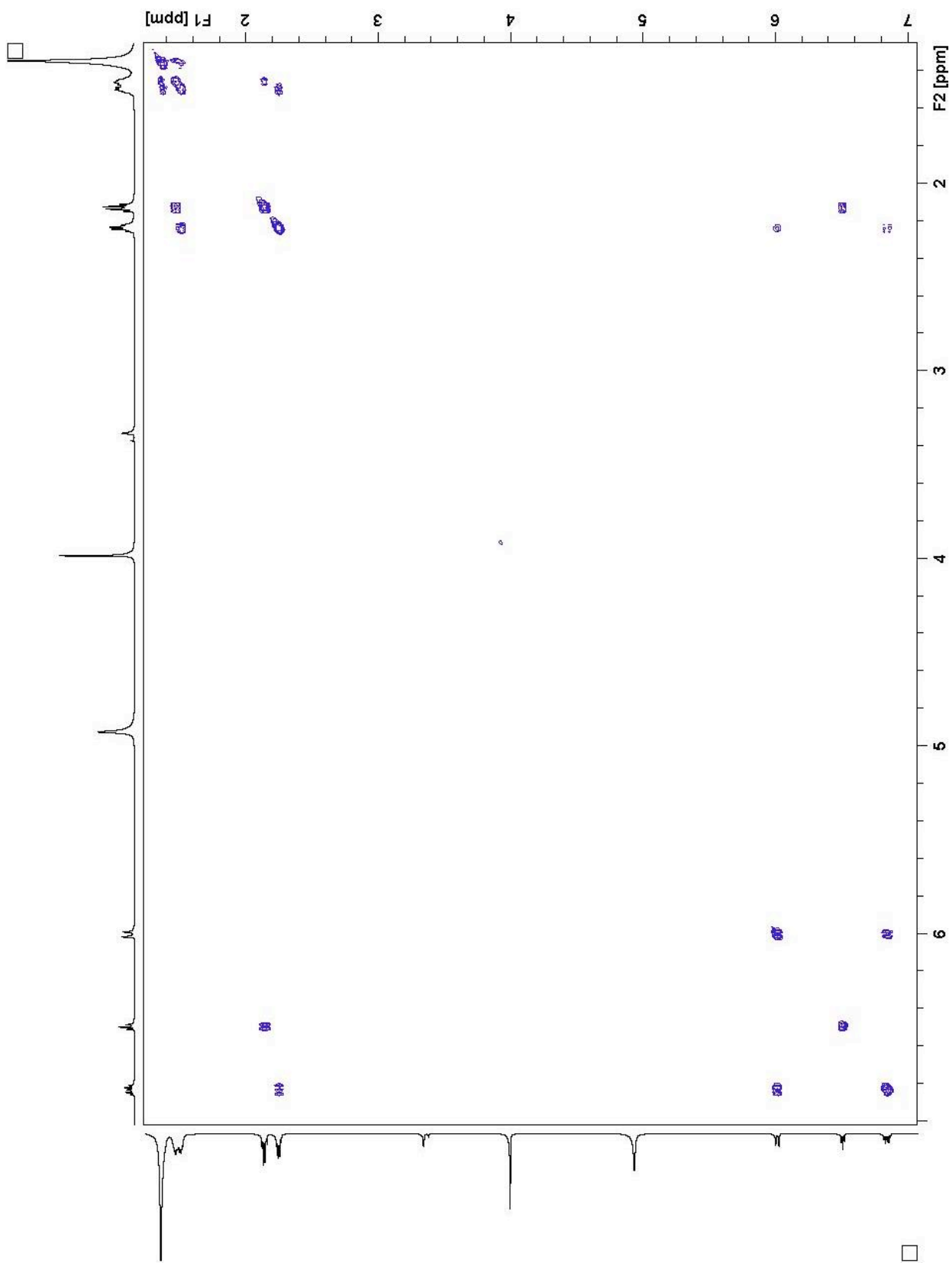


Figure S6. COSY spectrum of motualevic acid A (**1**) in CD₃OD.

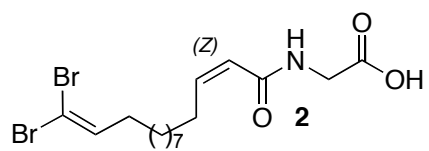
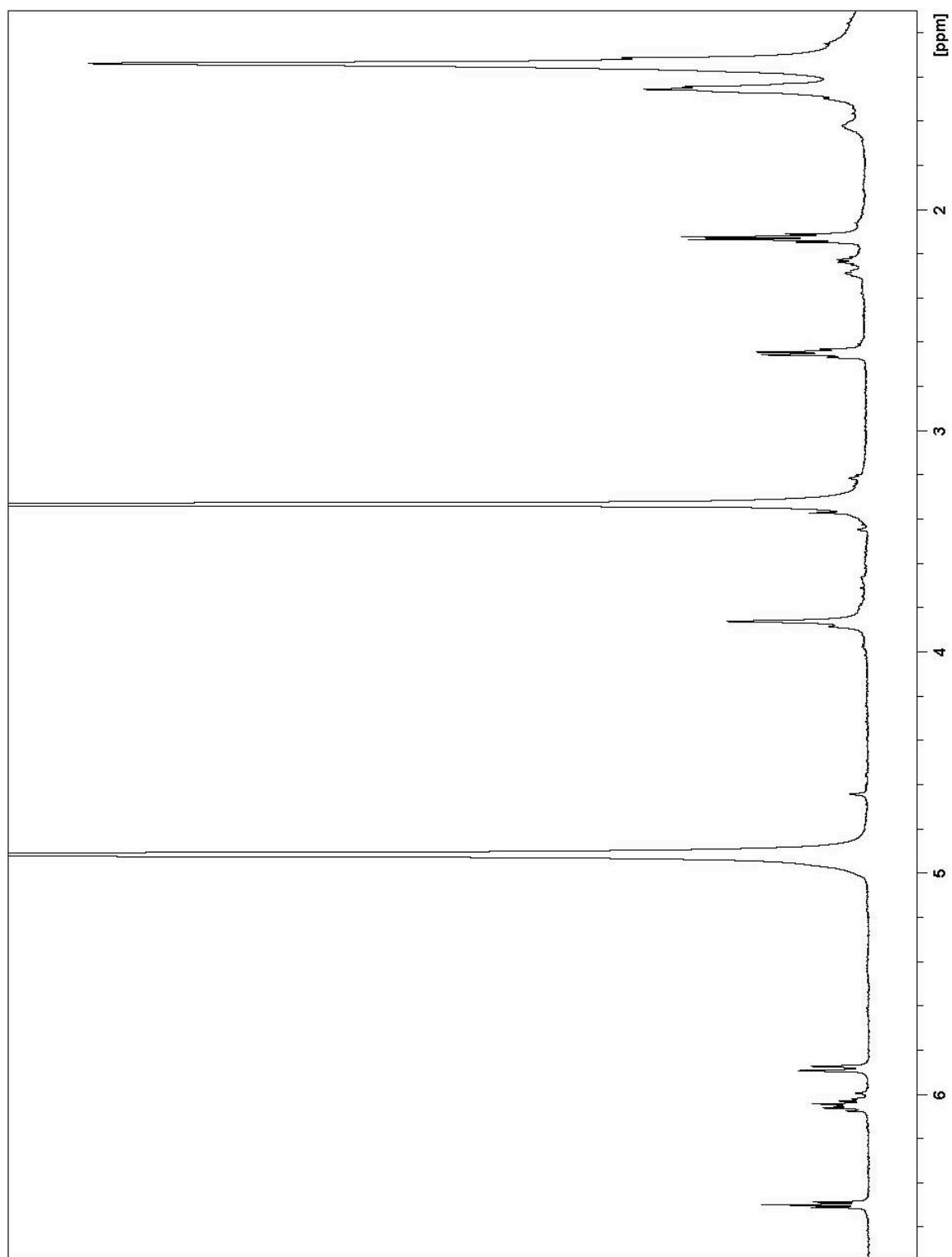


Figure S7. ^1H NMR spectrum of motualevic acid B (**2**) in CD_3OD .

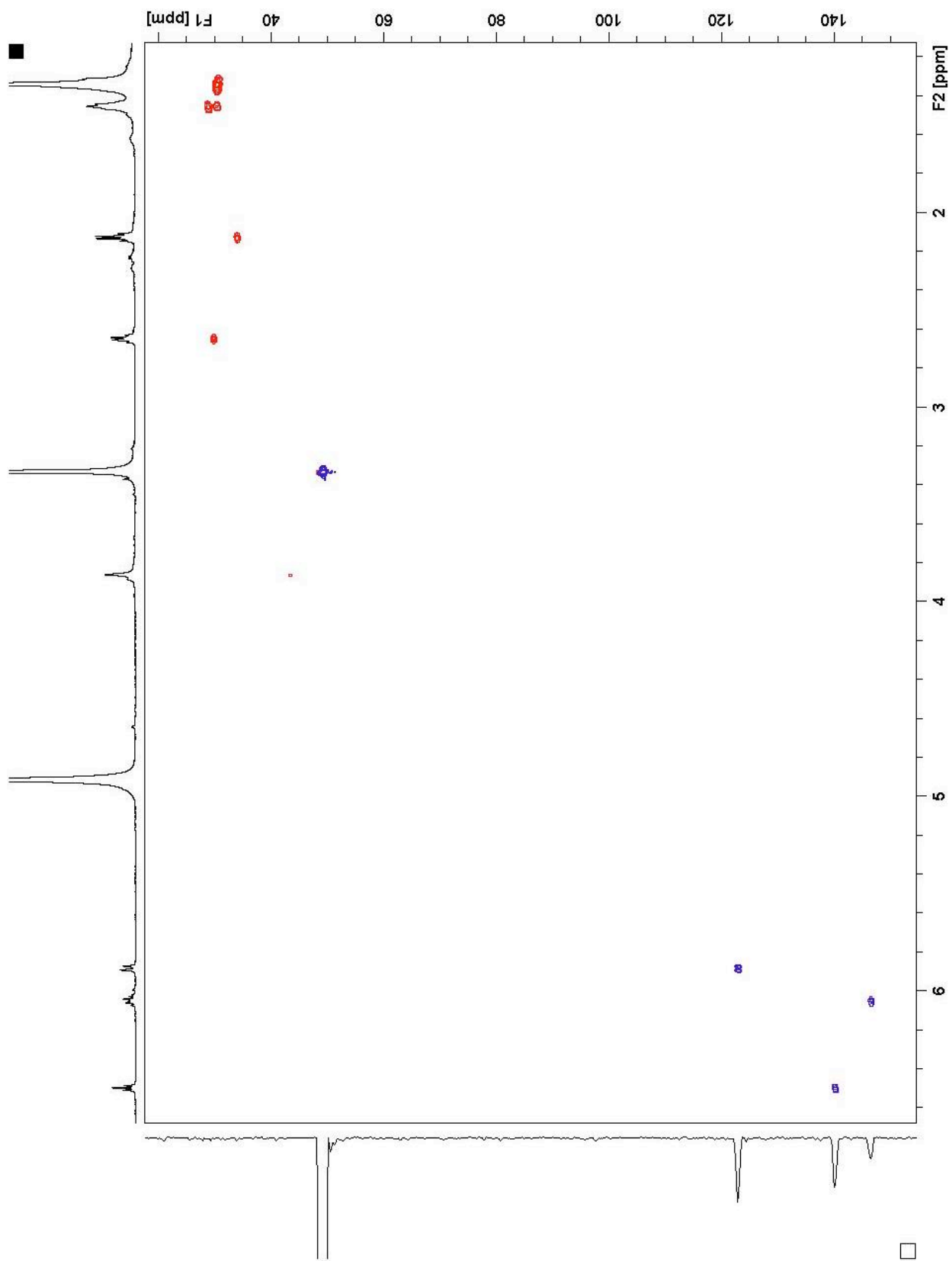


Figure S8. HSQC spectrum of motualevic acid B (**2**) in CD₃OD.

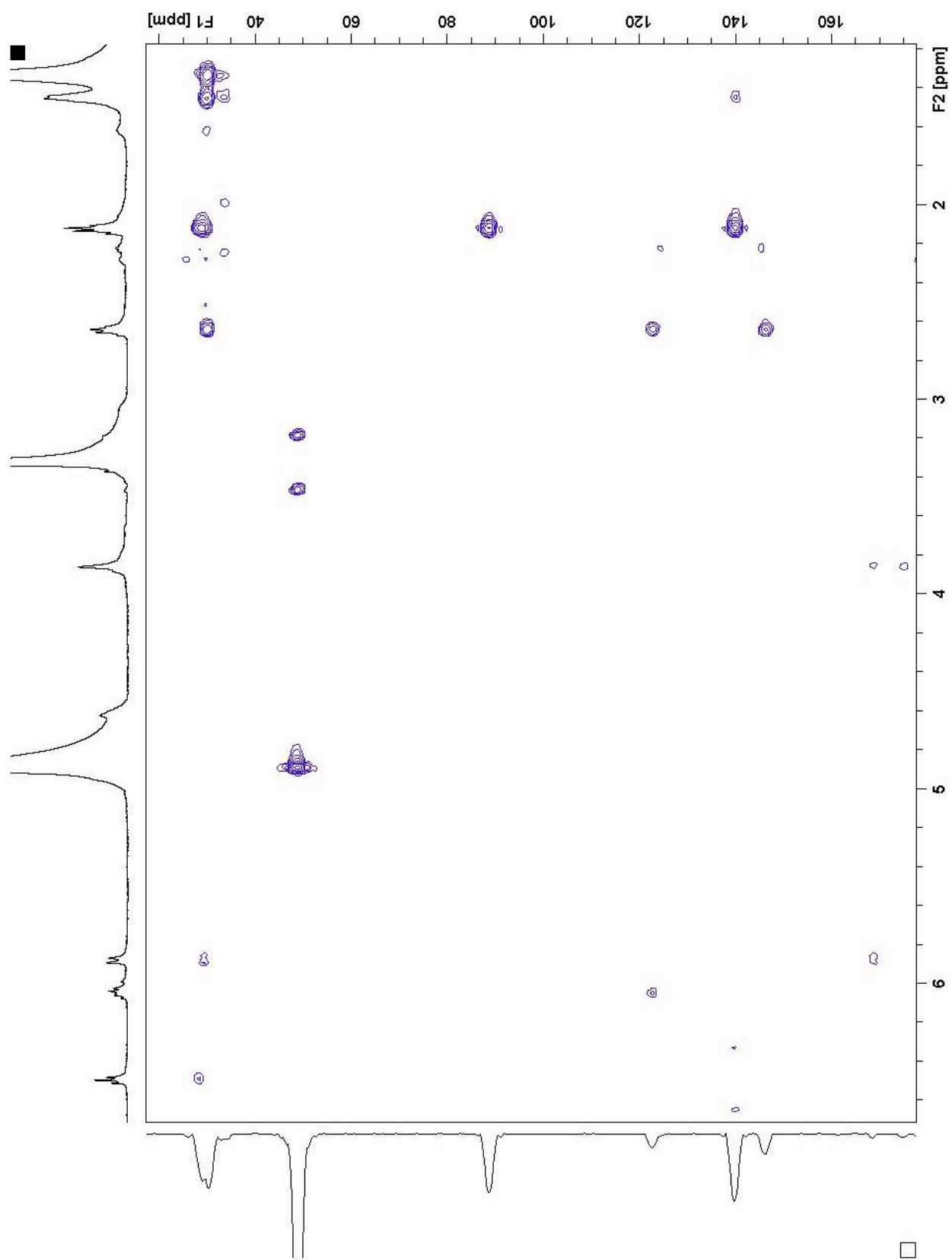


Figure S9. HMBC spectrum of motualevic acid B (2) in CD₃OD.

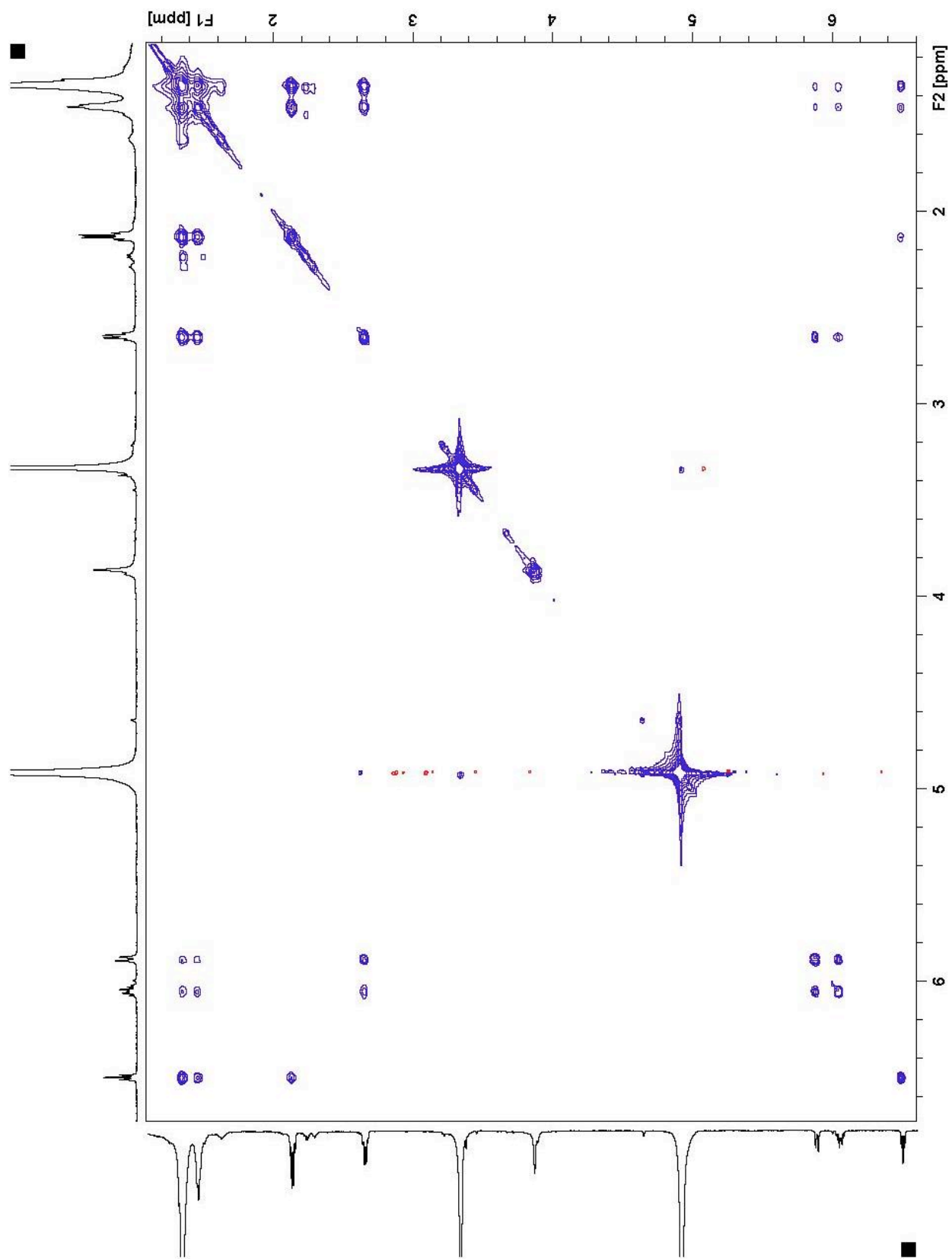


Figure S10. TOCSY spectrum of motualevic acid B (**2**) in CD₃OD.

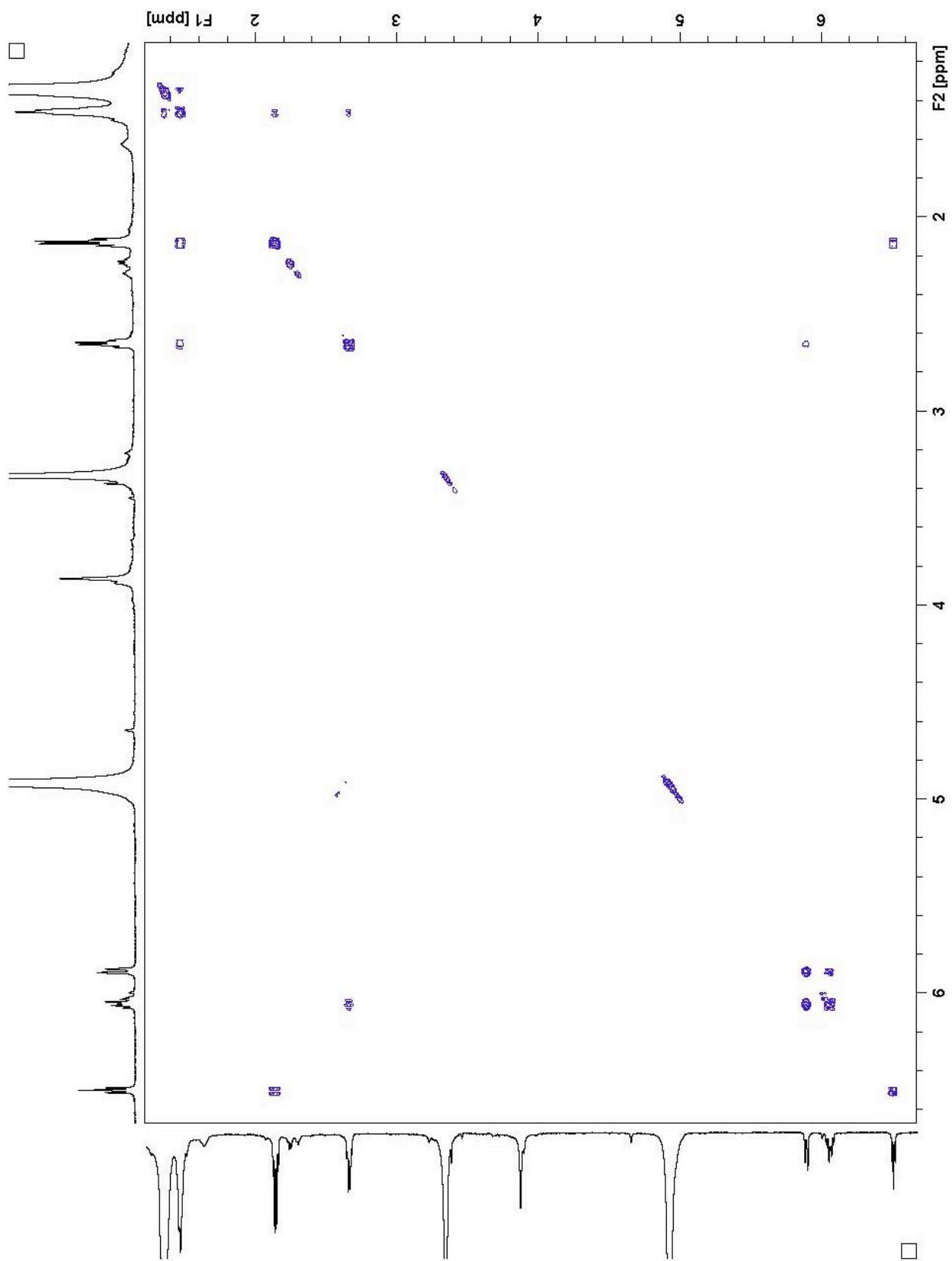


Figure S11. COSY spectrum of motualevic acid B (**2**) in CD₃OD.

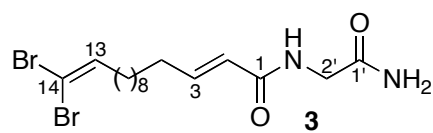
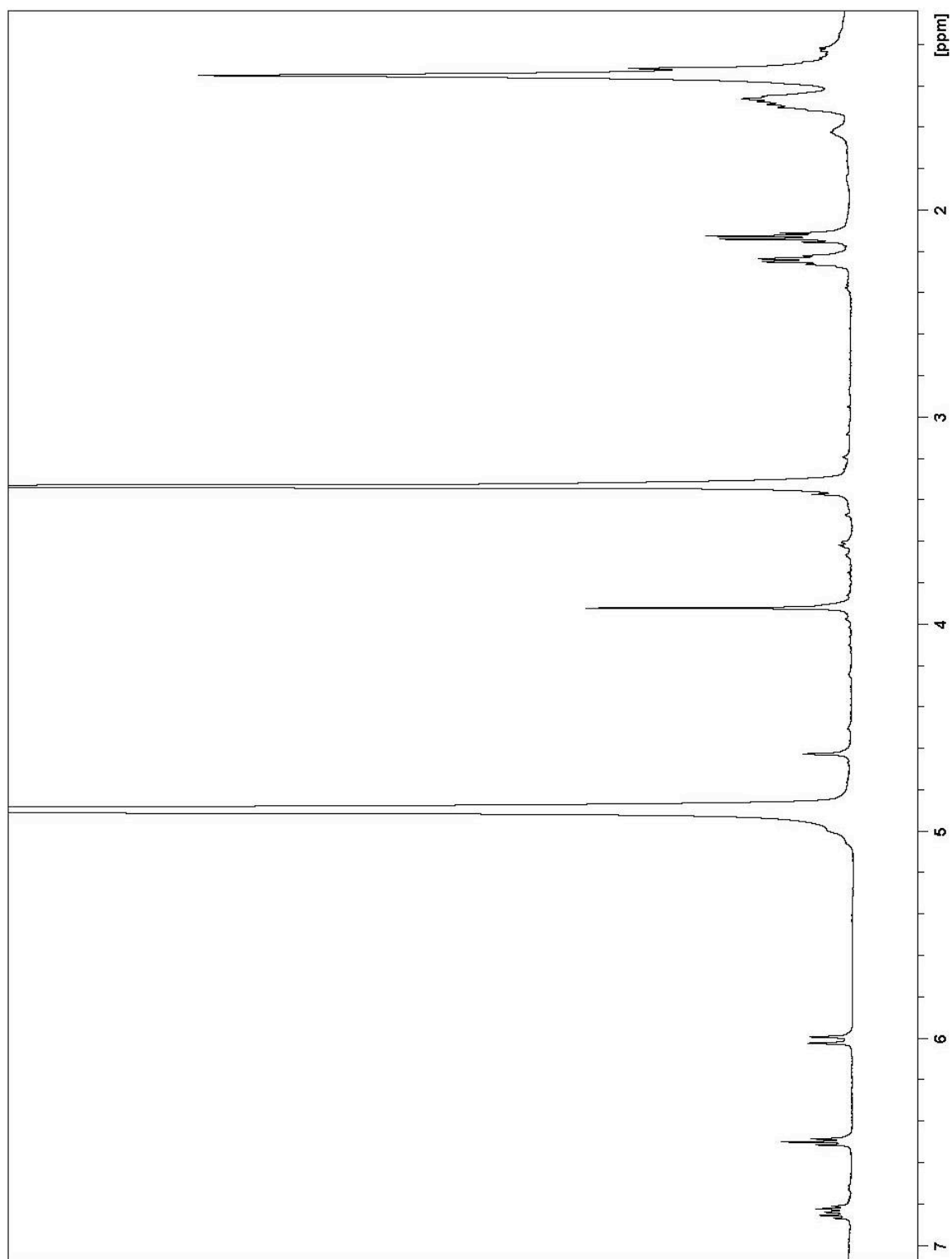


Figure S12. ¹H NMR spectrum of motualevic acid C (**3**) in CD₃OD.

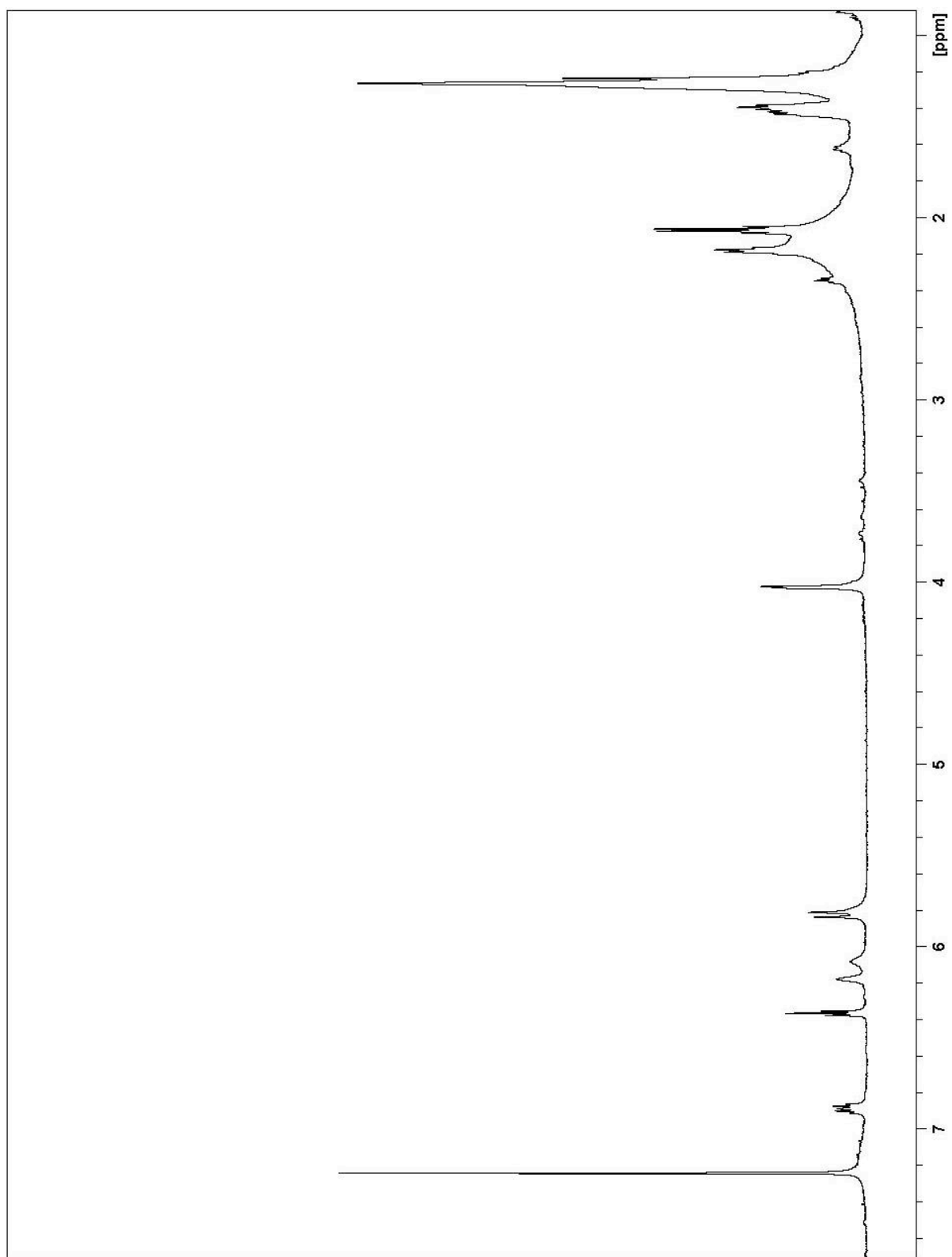


Figure S13. ^1H NMR spectrum of motualevic acid C (**3**) in CDCl_3 .

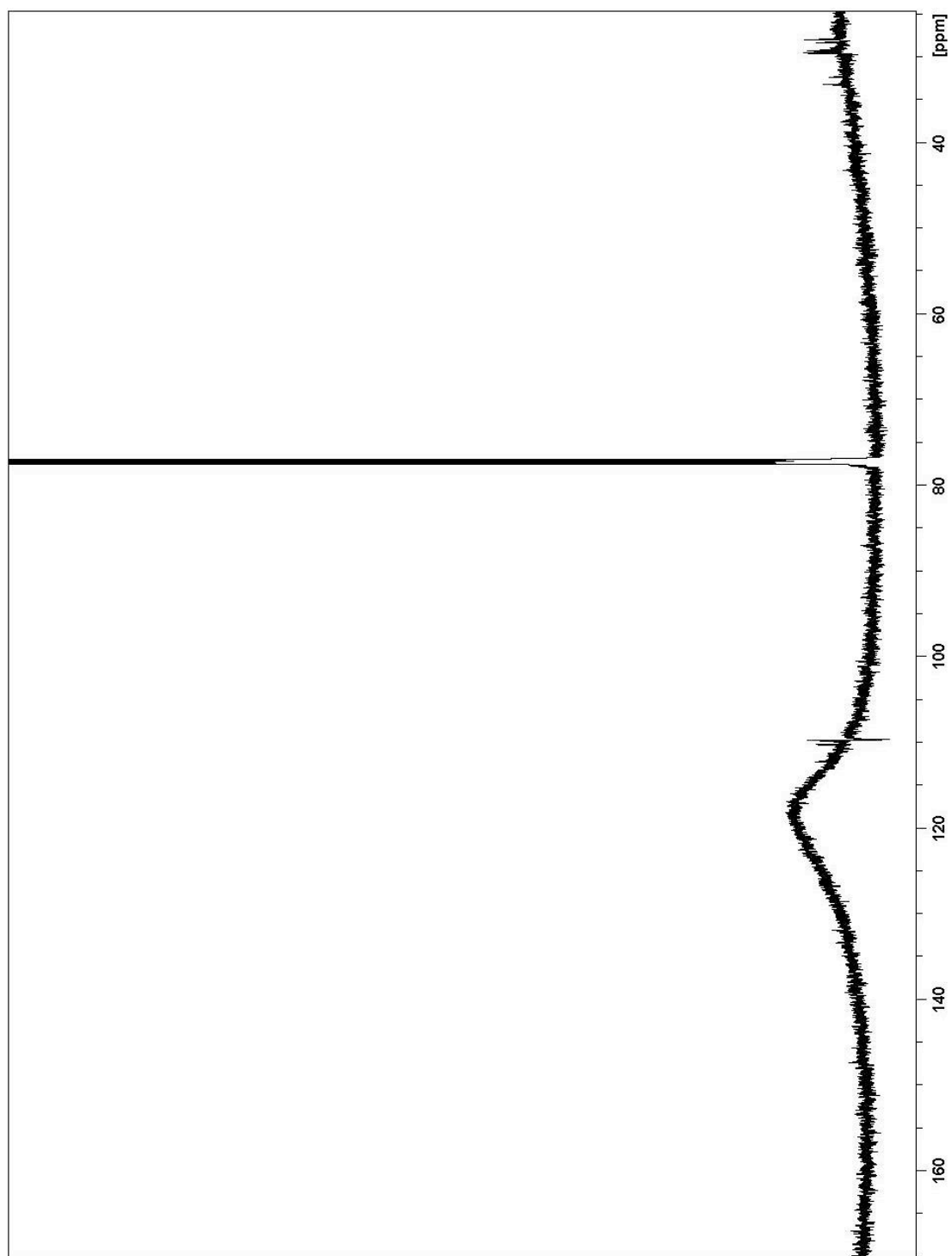


Figure S14. ^{13}C NMR spectrum of motualevic acid C (3) in CDCl_3 .

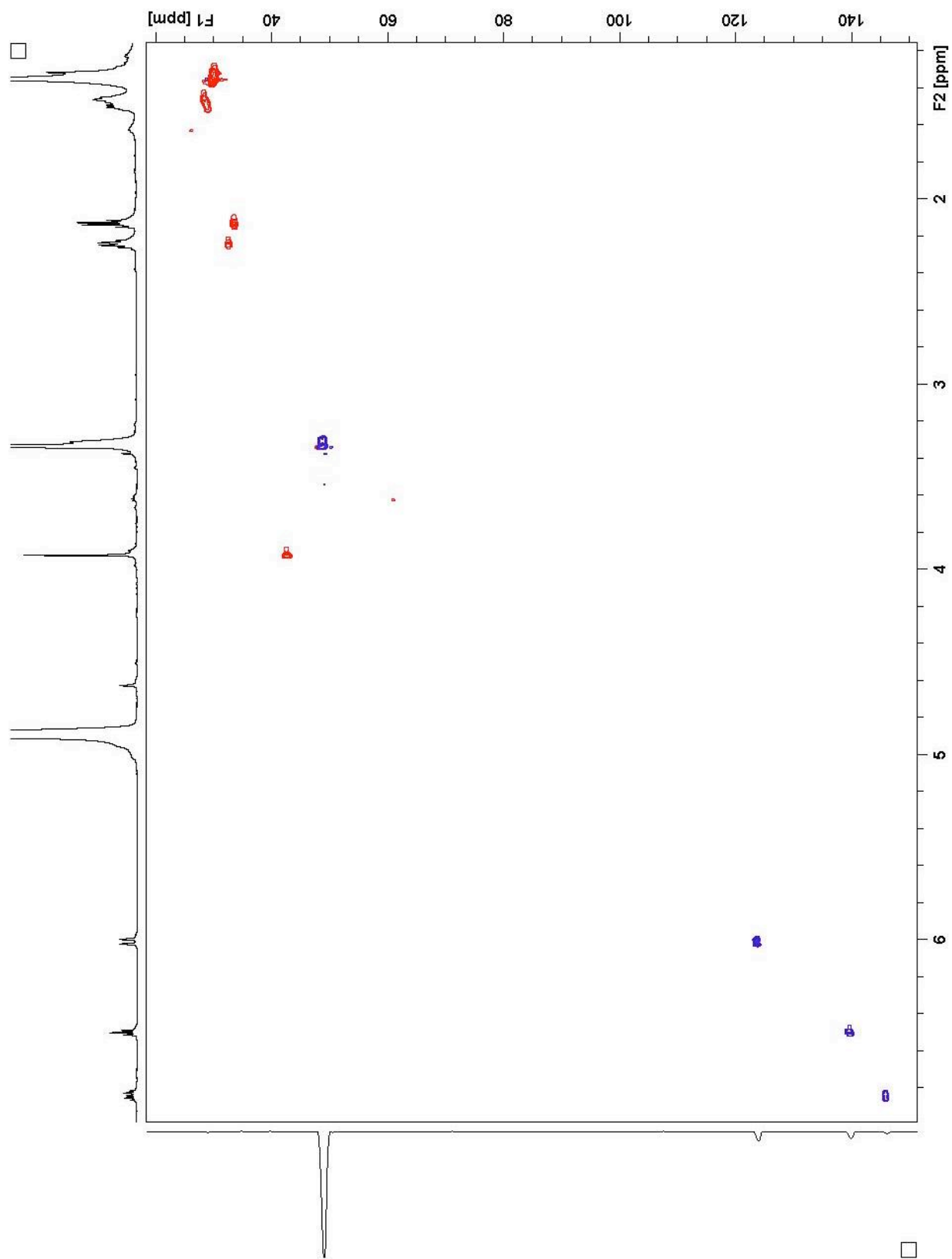


Figure S15. HSQC spectrum of motualevic acid C (3) in CD₃OD.

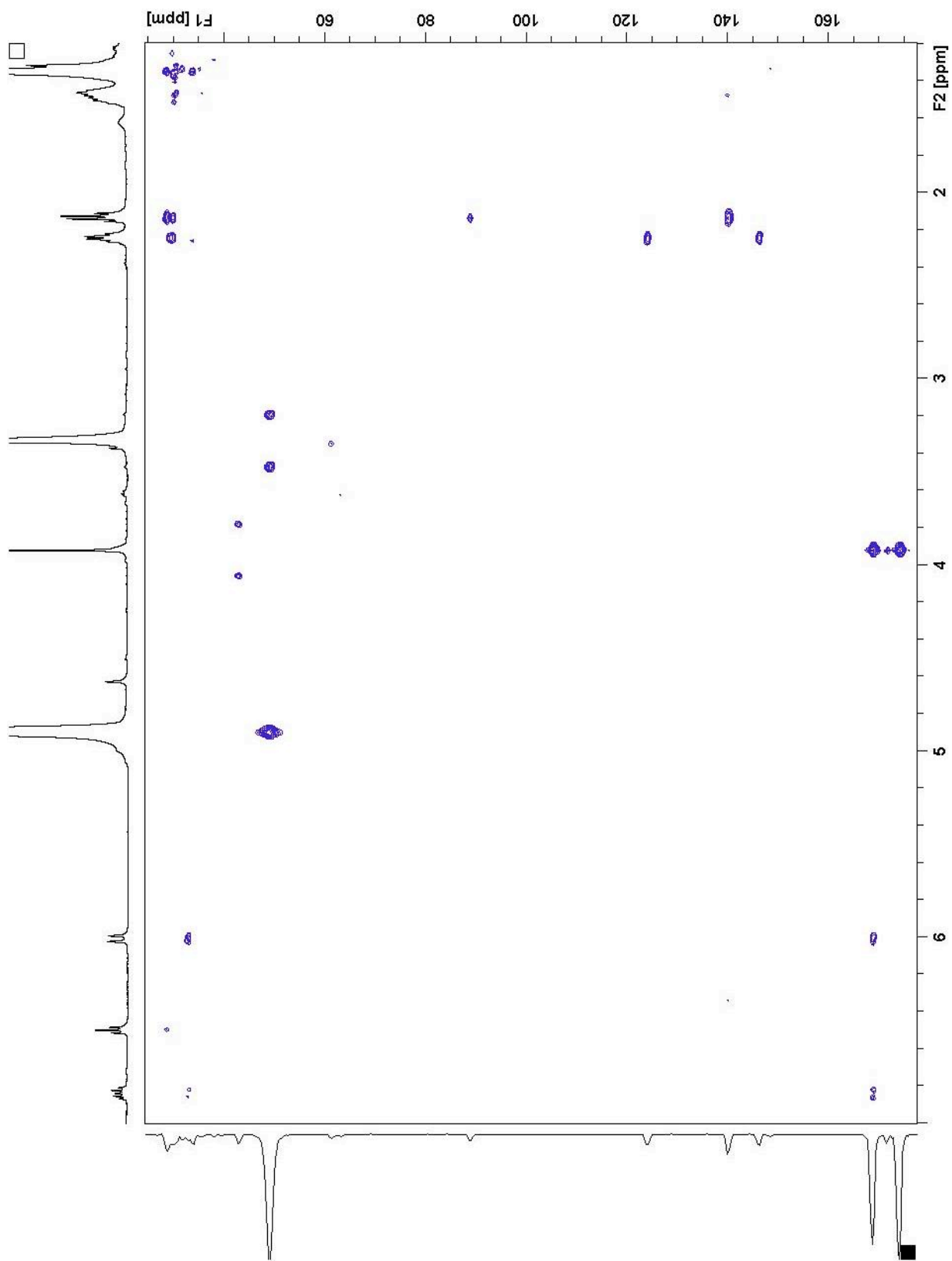


Figure S16. HMBC spectrum of motualevic acid C (**3**) in CD₃OD.

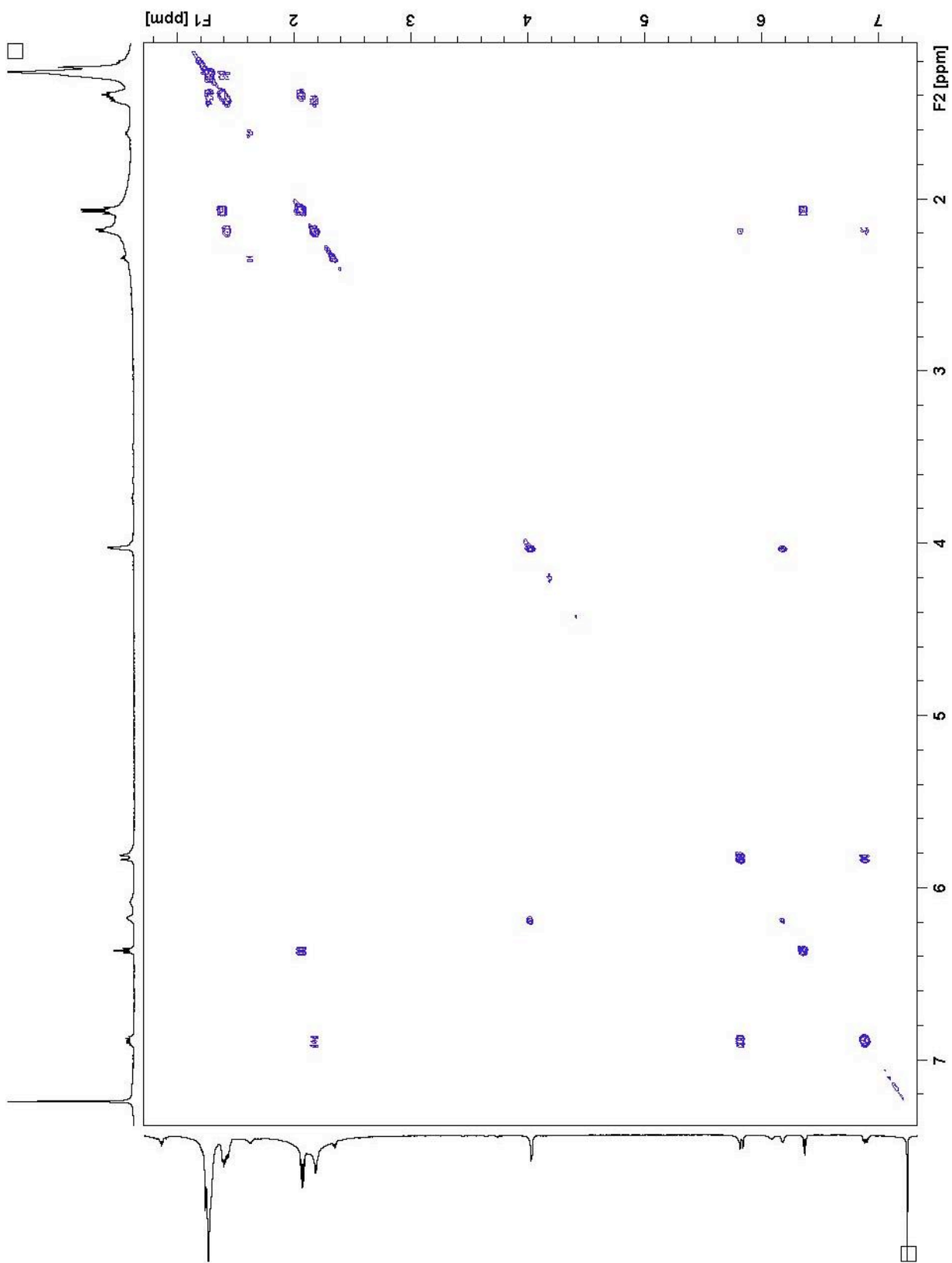


Figure S17. COSY spectrum of motualevic acid C (**3**) in CDCl₃.

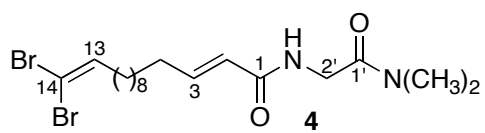
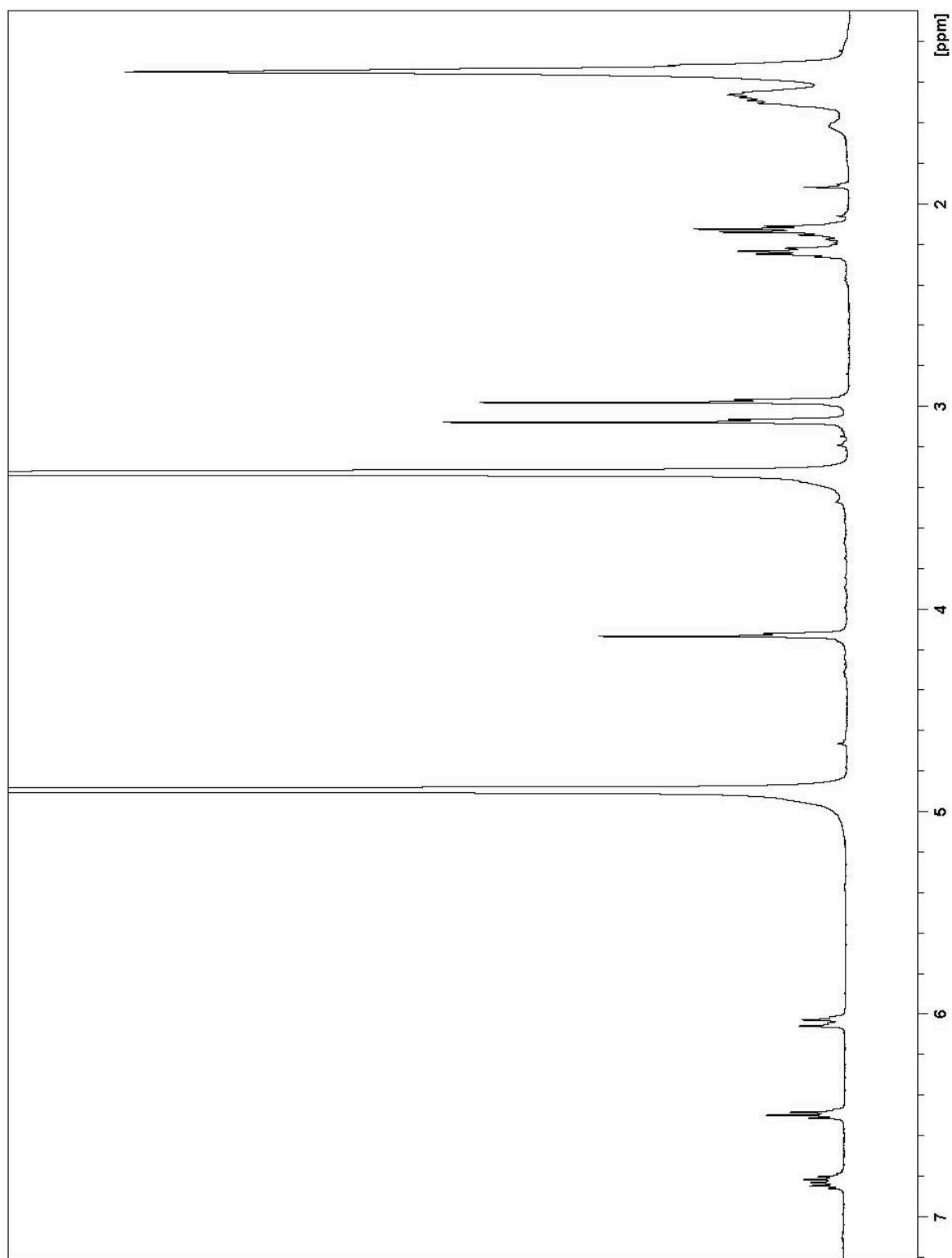


Figure S18. ¹H NMR spectrum of motualevic acid D (**4**) in CD₃OD.

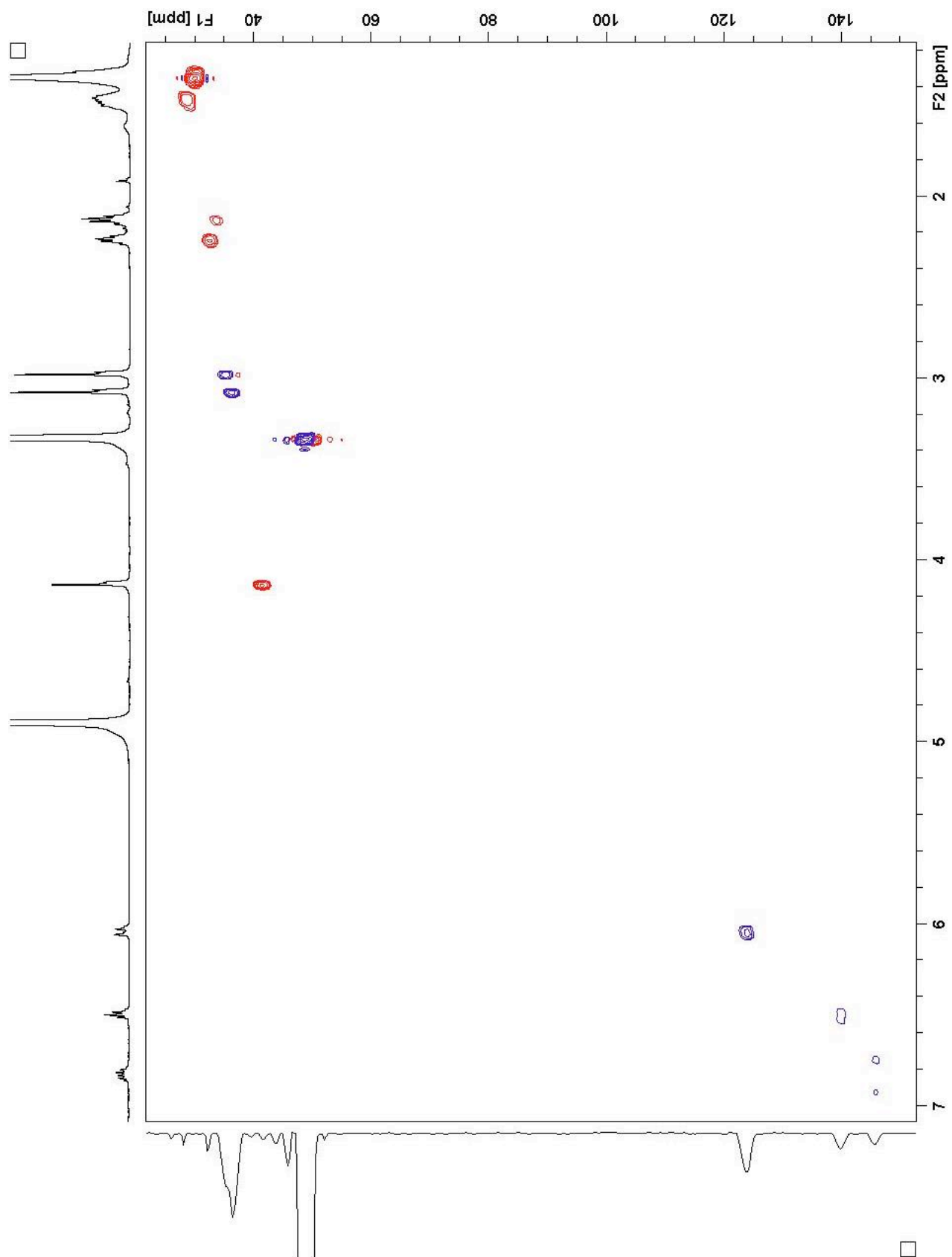


Figure S19. HSQC spectrum of motualevic acid D (4) in CD₃OD.

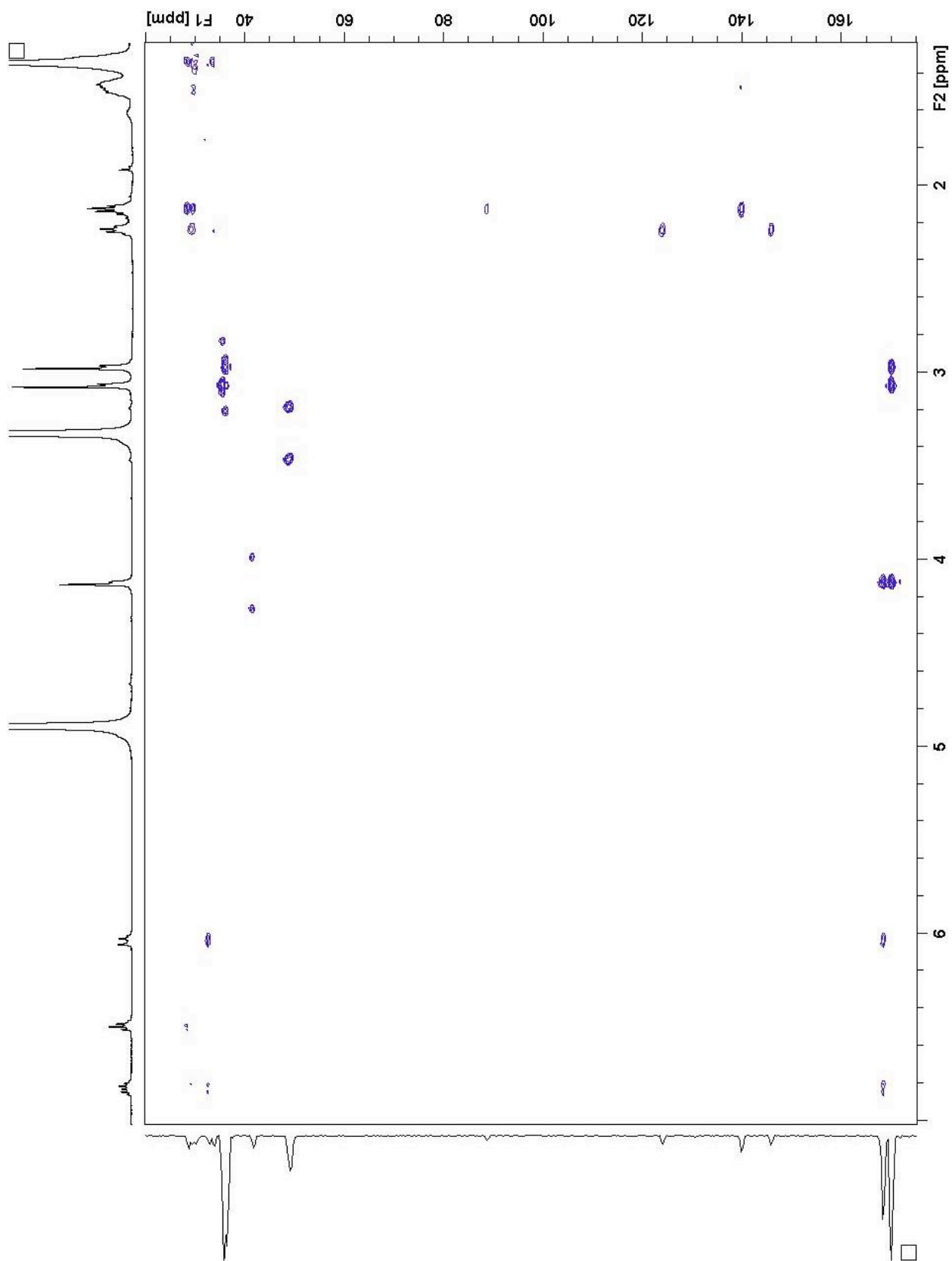


Figure S20. HMBC spectrum of motualevic acid D (4) in CD₃OD.

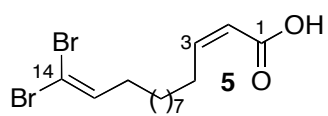
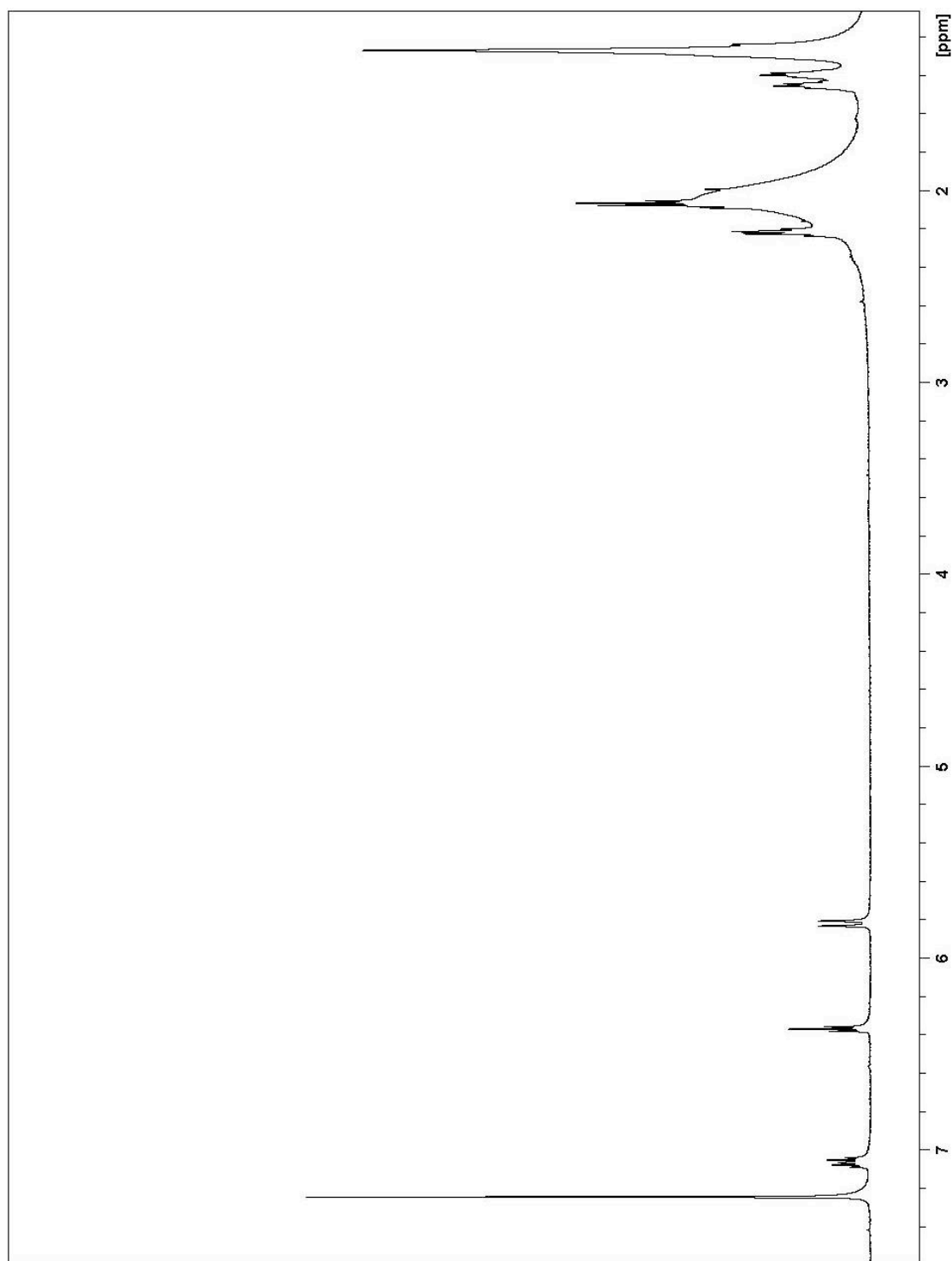


Figure S21. ¹H NMR spectrum of motualevic acid E (**5**) in CDCl₃.

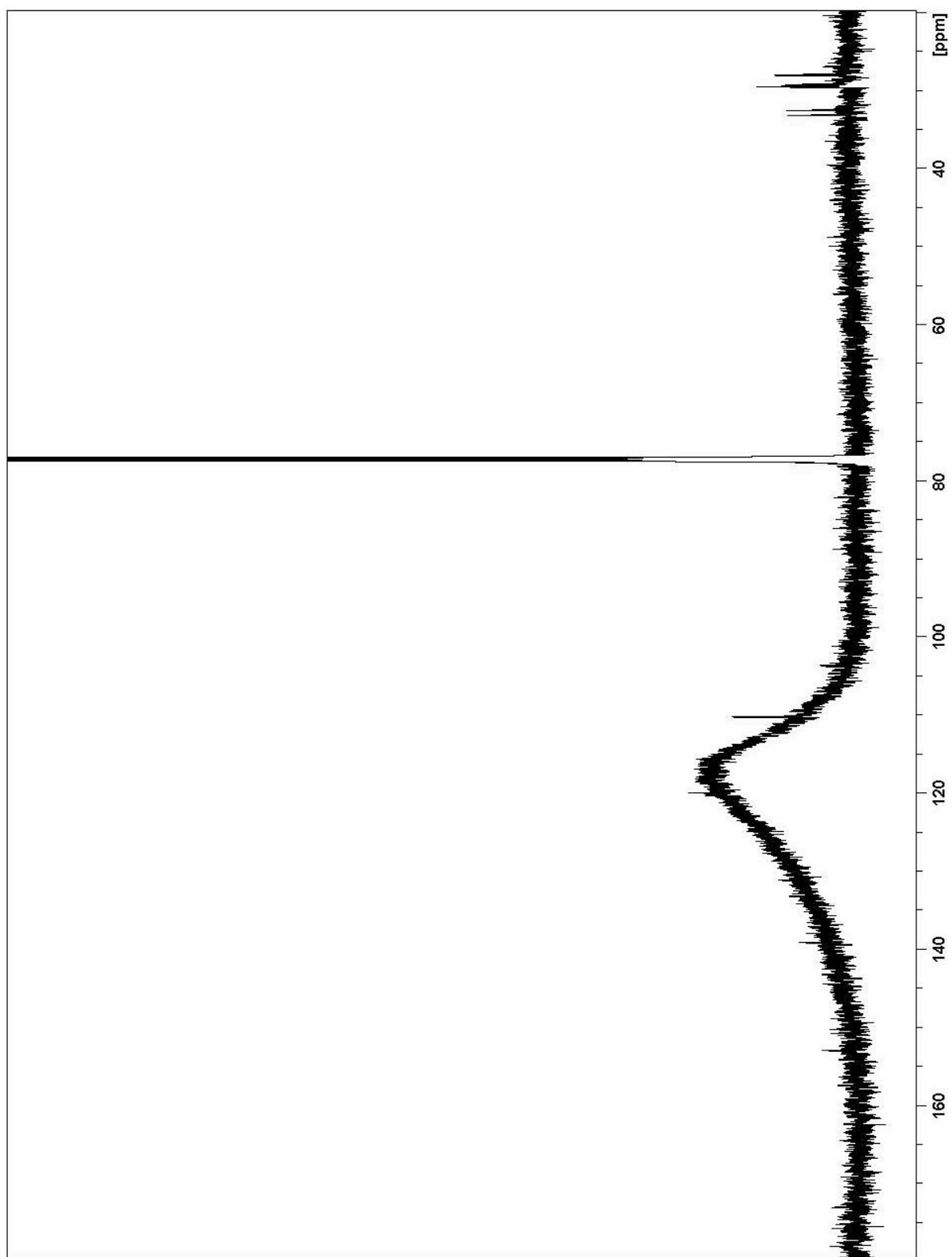


Figure S22. ^{13}C NMR spectrum of motualevic acid E (5) in CDCl_3

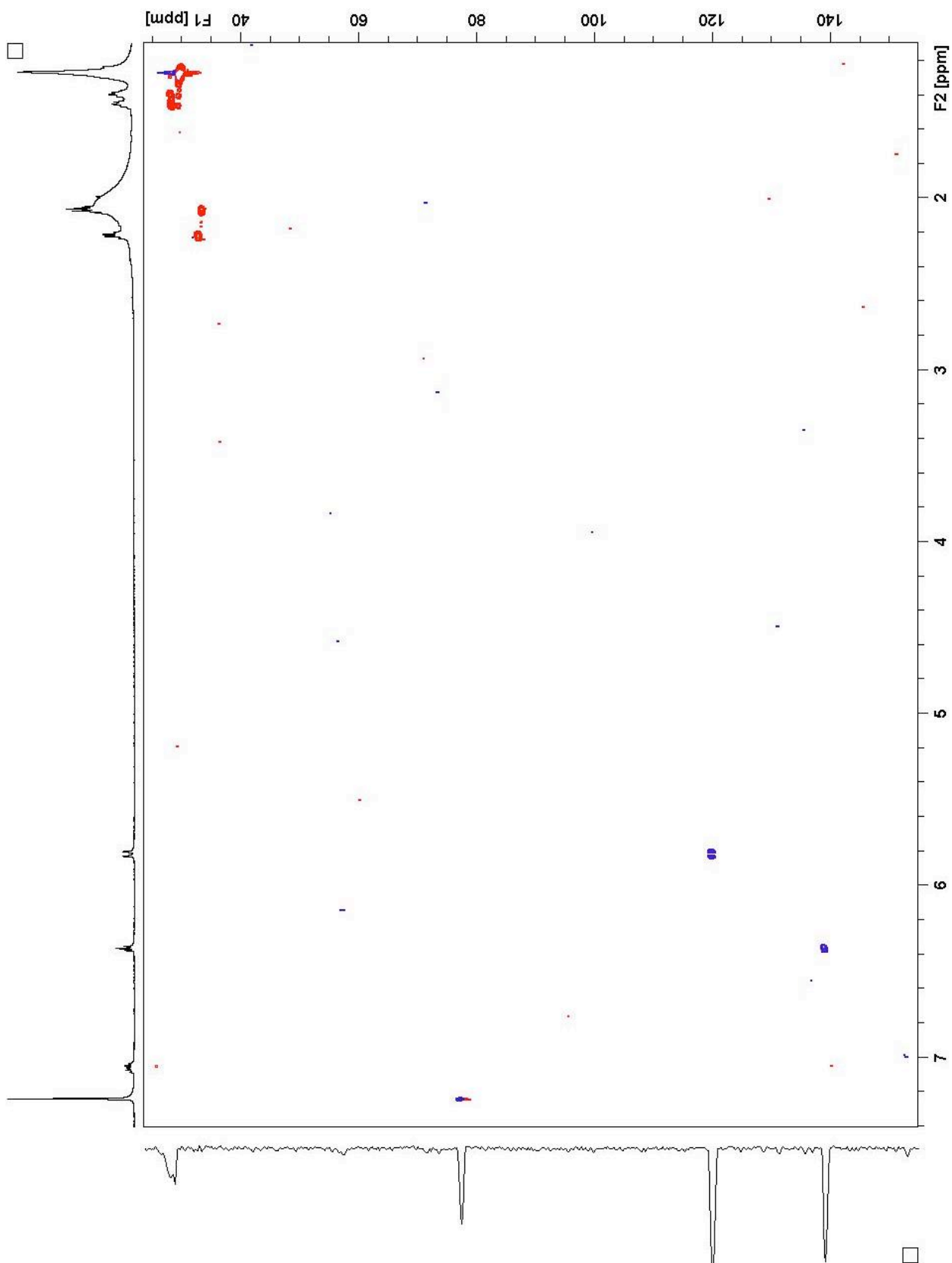


Figure S23. HSQC spectrum of motualevic acid E (**5**) in CDCl₃.

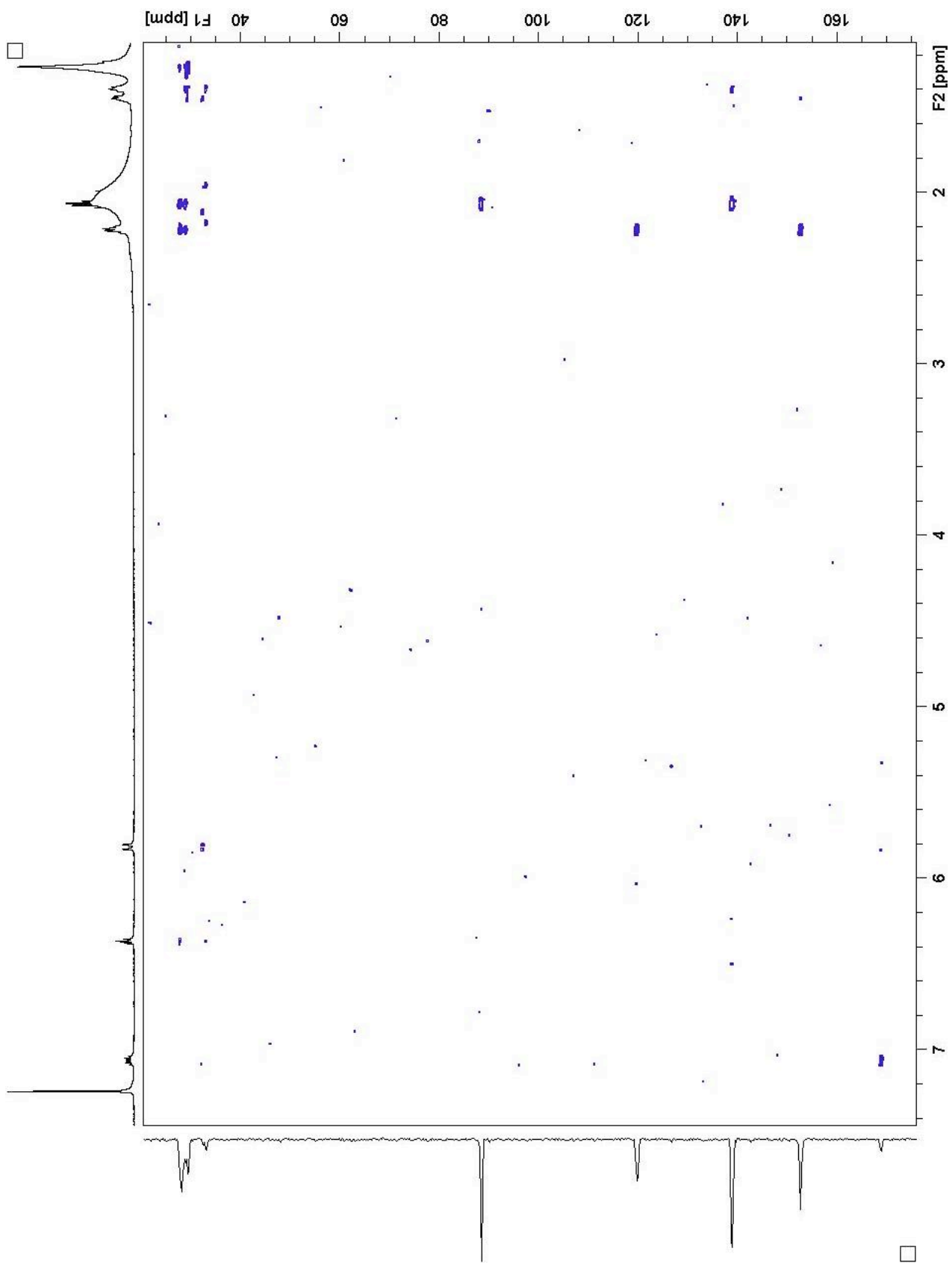


Figure S24. HMBC spectrum of motualevic acid E (5) in CDCl₃.

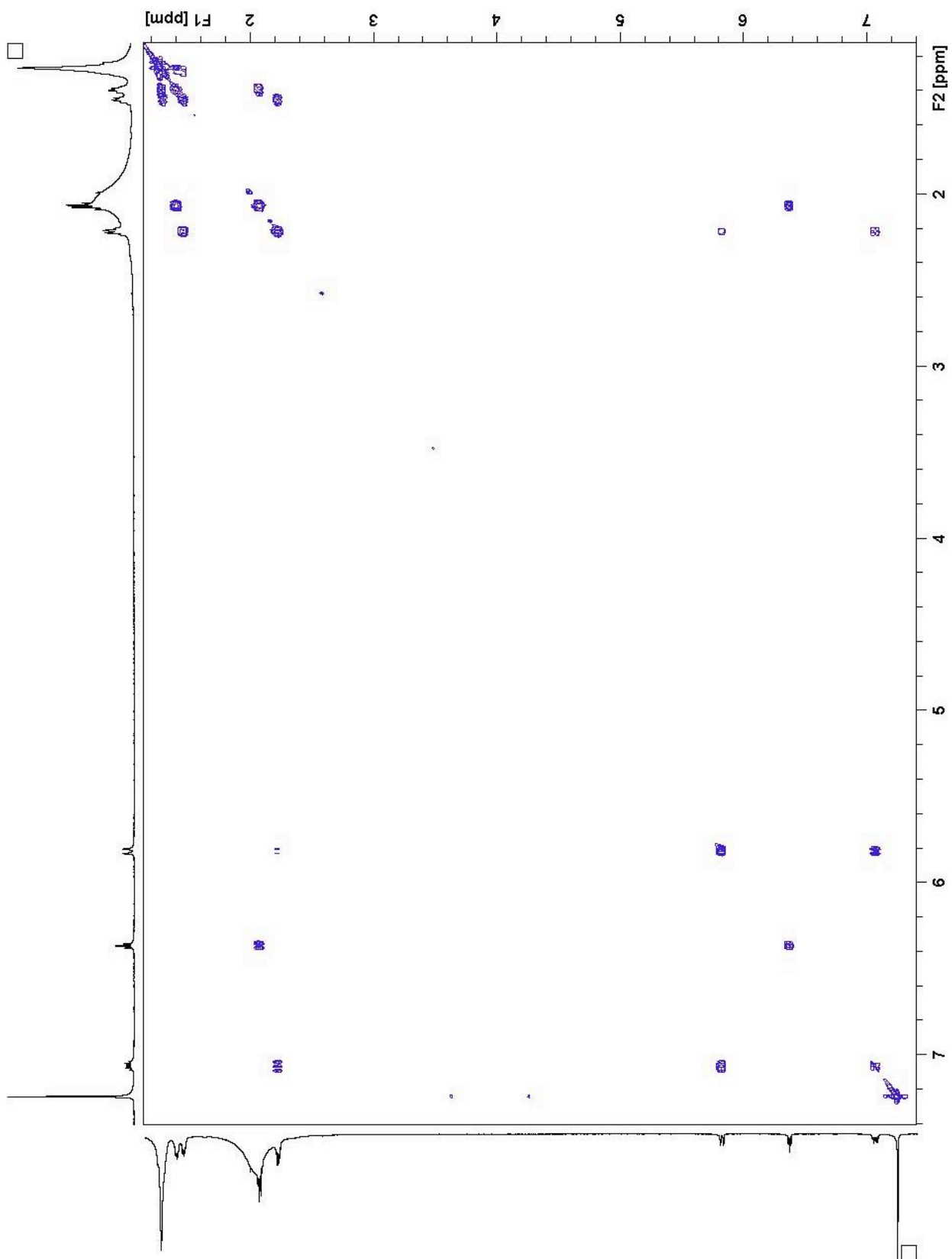


Figure S25. COSY spectrum of motualevic acid E (**5**) in CDCl₃.

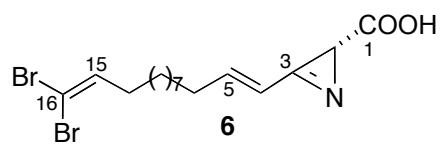
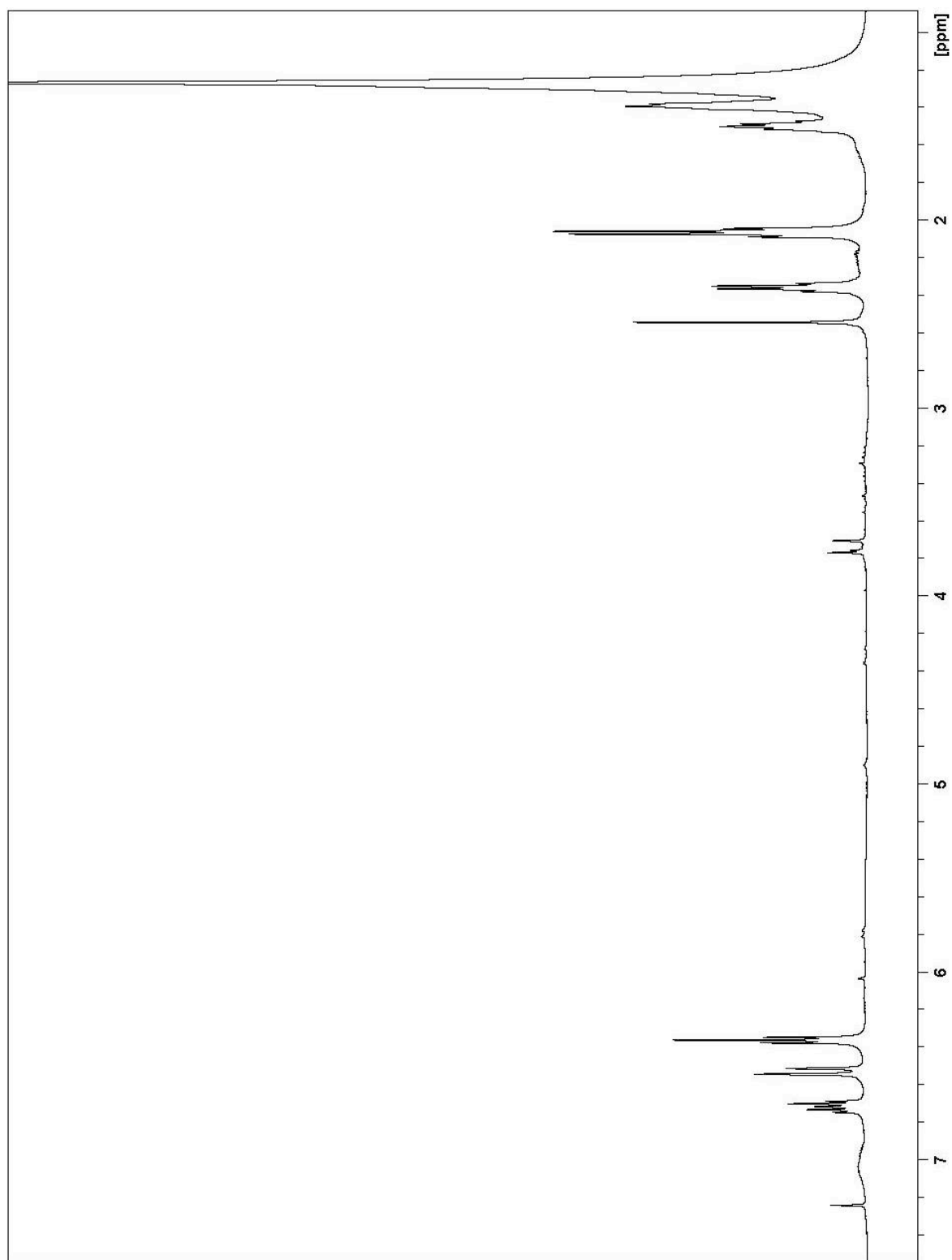


Figure S26. ^1H NMR spectrum of motualevic acid F (**6**) in CDCl_3 .

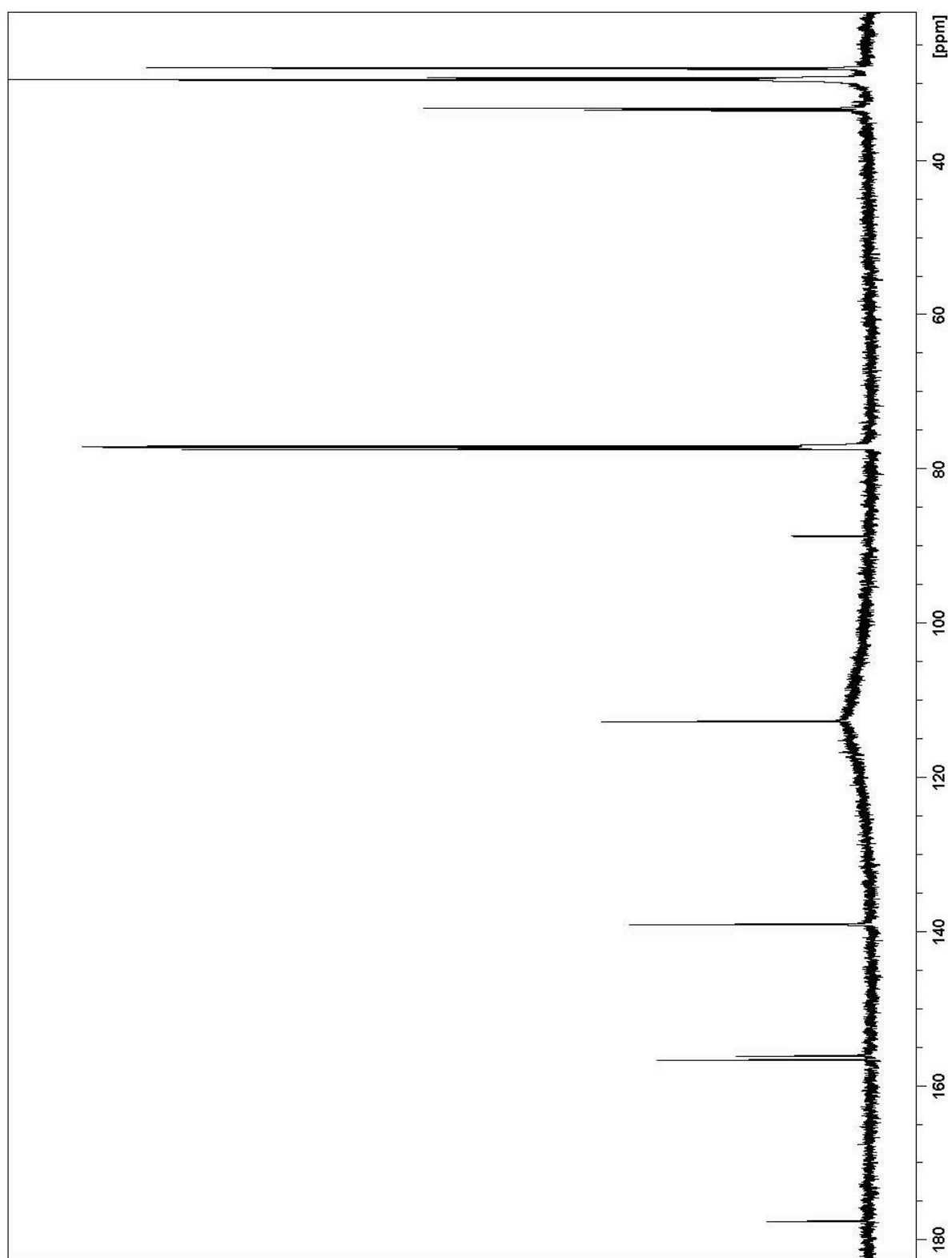


Figure S27. ^{13}C spectrum of motualevic acid F (**6**) in CDCl_3 .

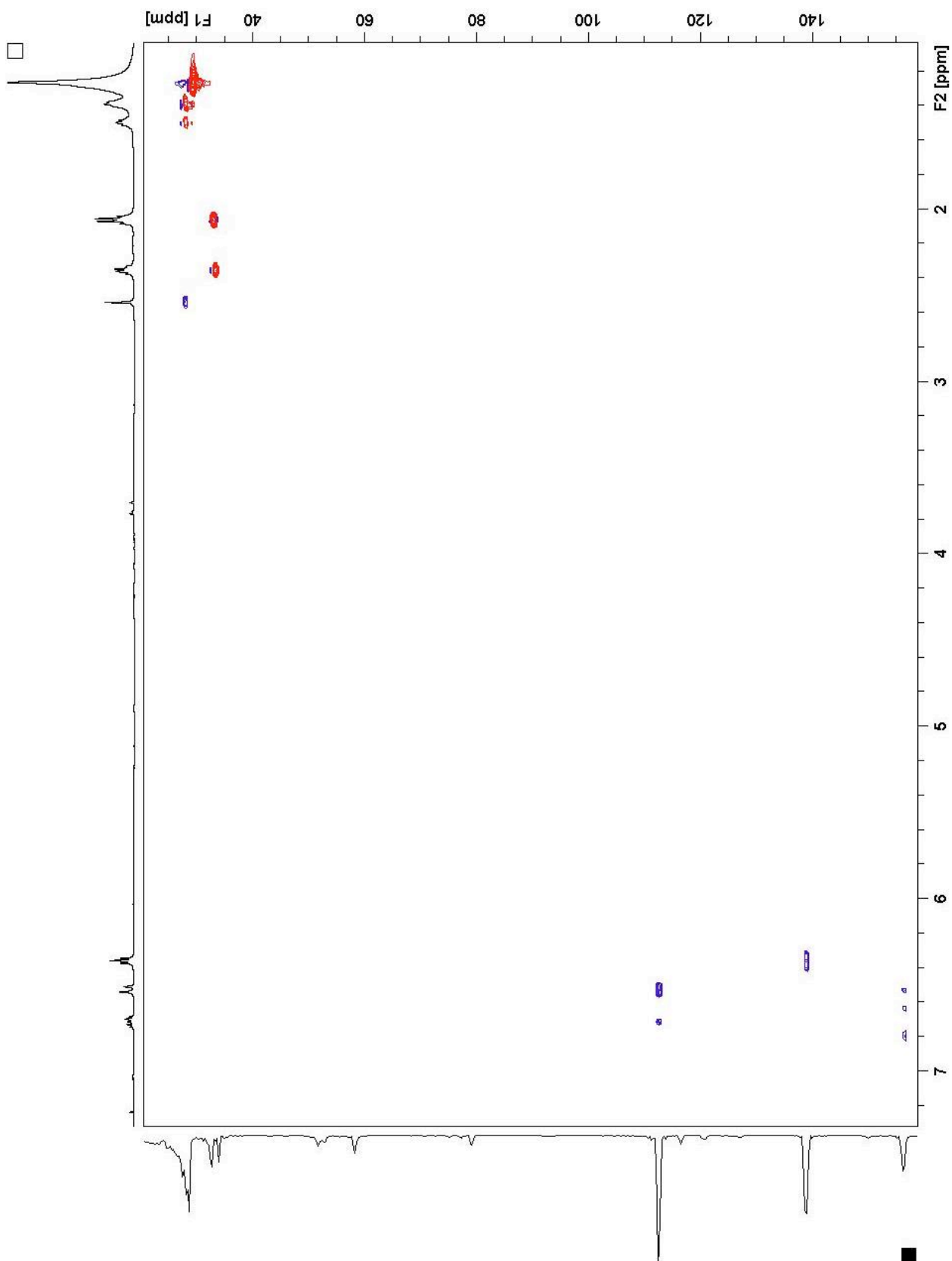


Figure S28. HSQC spectrum of motualevic acid F (**6**) in CDCl_3 .

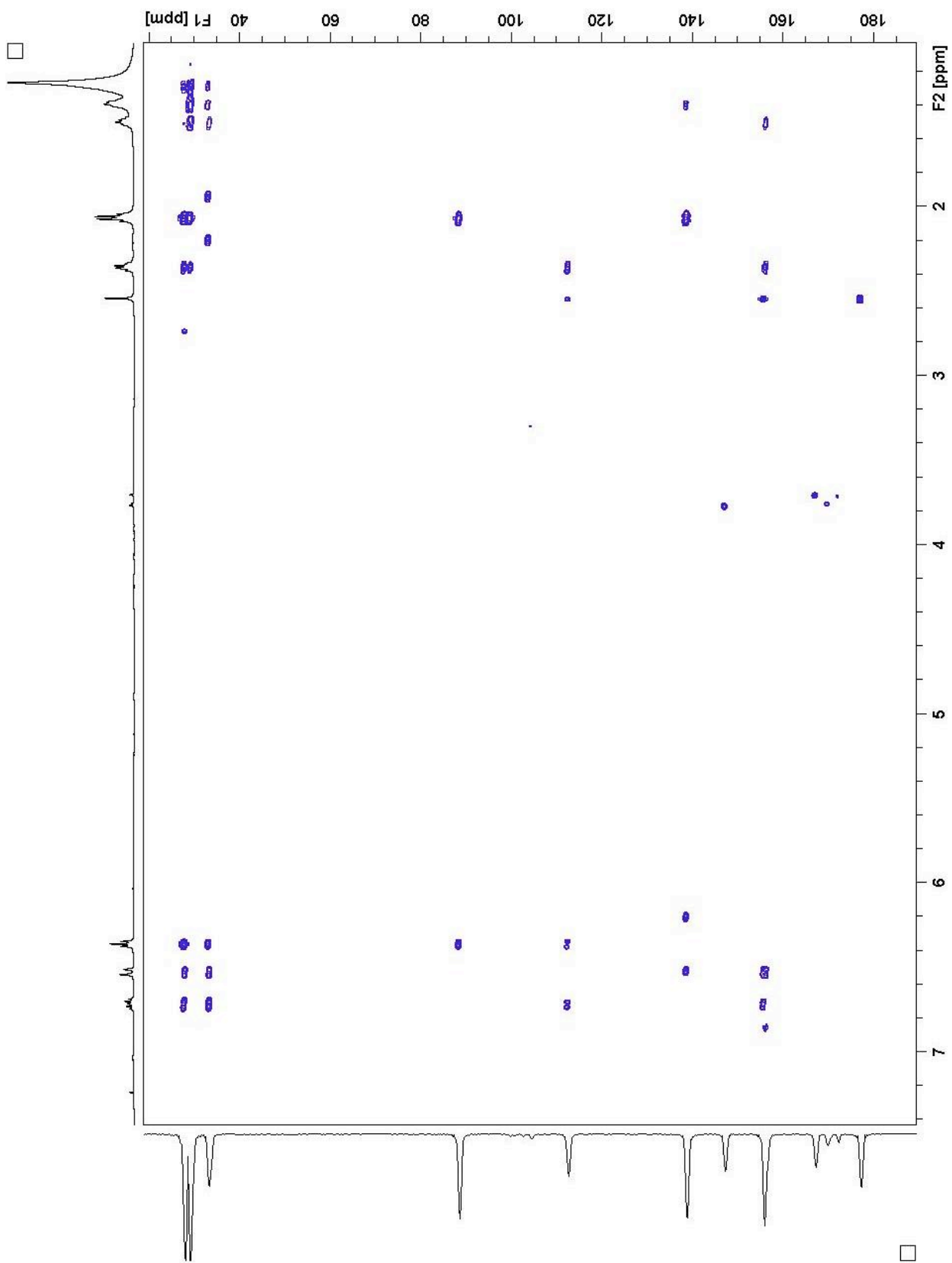


Figure S29. HMBC spectrum of motualevic acid F (**6**) in CDCl_3 .

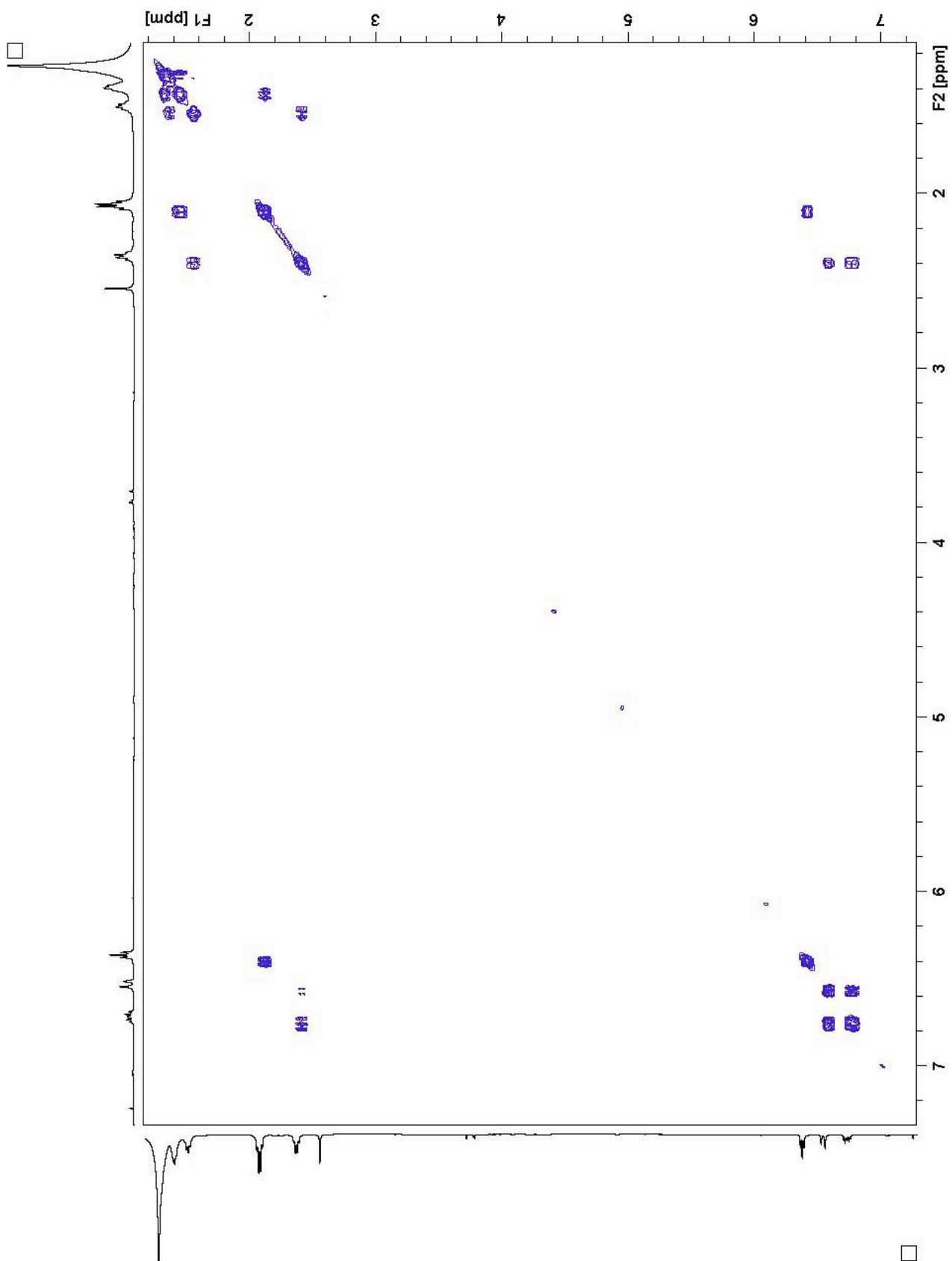


Figure S30. COSY spectrum of motualevic acid F (**6**) in CDCl₃.

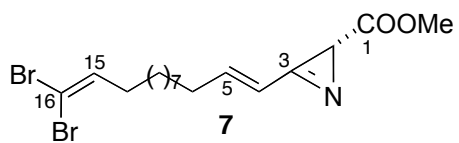
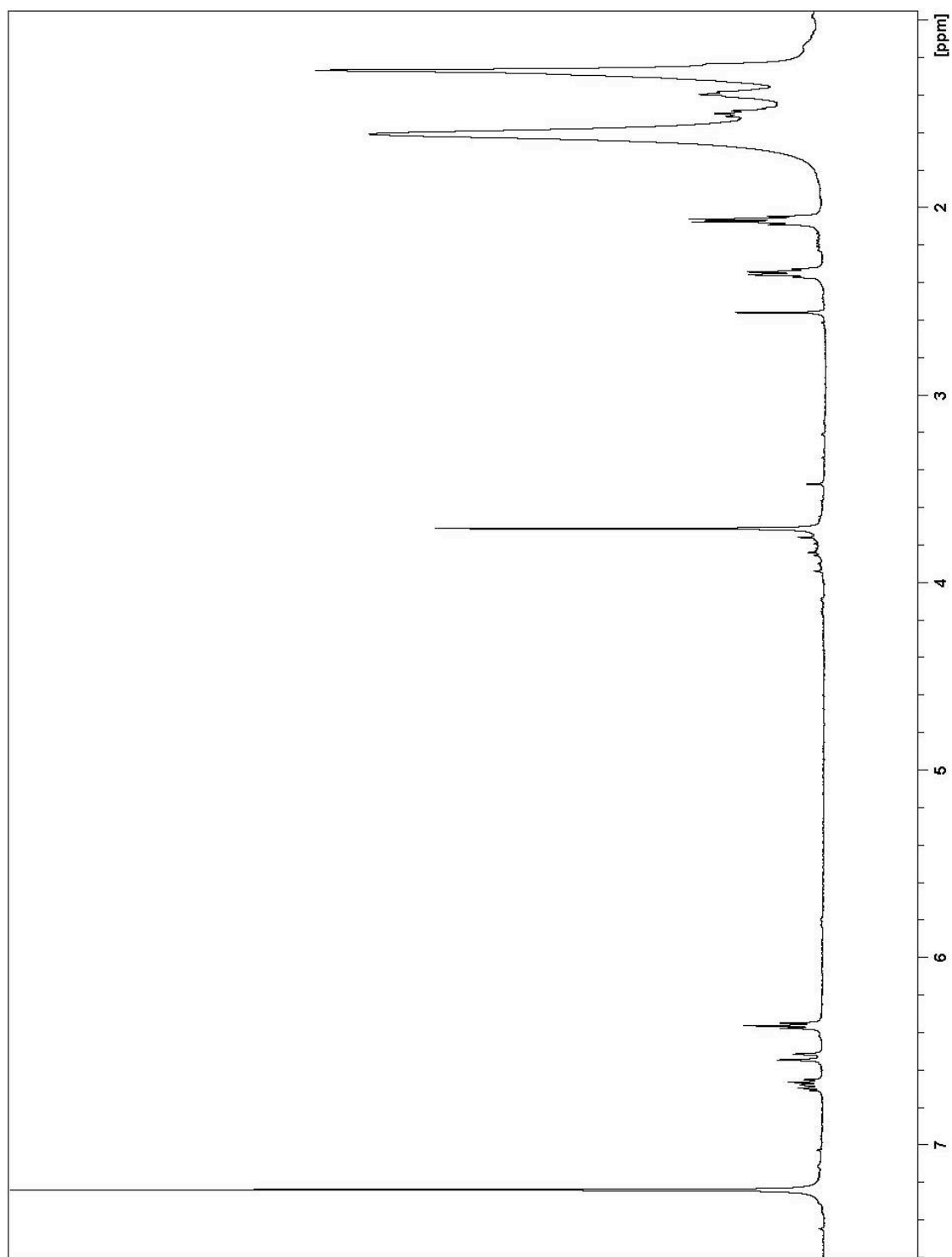


Figure S31. ^1H spectrum of (4*E*)-*R*-antazarine (**7**) in CDCl_3 .

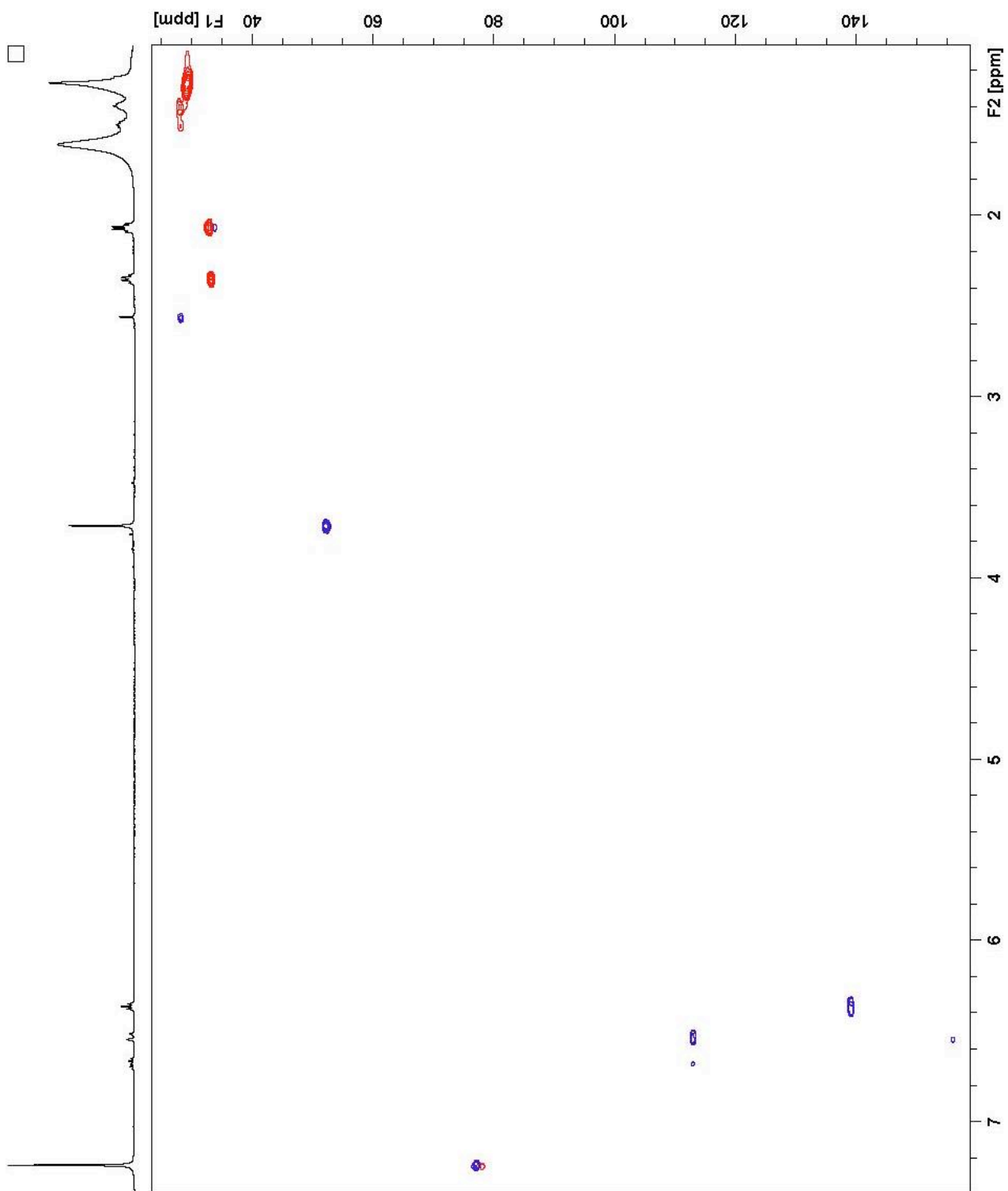


Figure S32. HSQC spectrum of (4*E*)-*R*-antazarine (**7**) in CDCl₃.

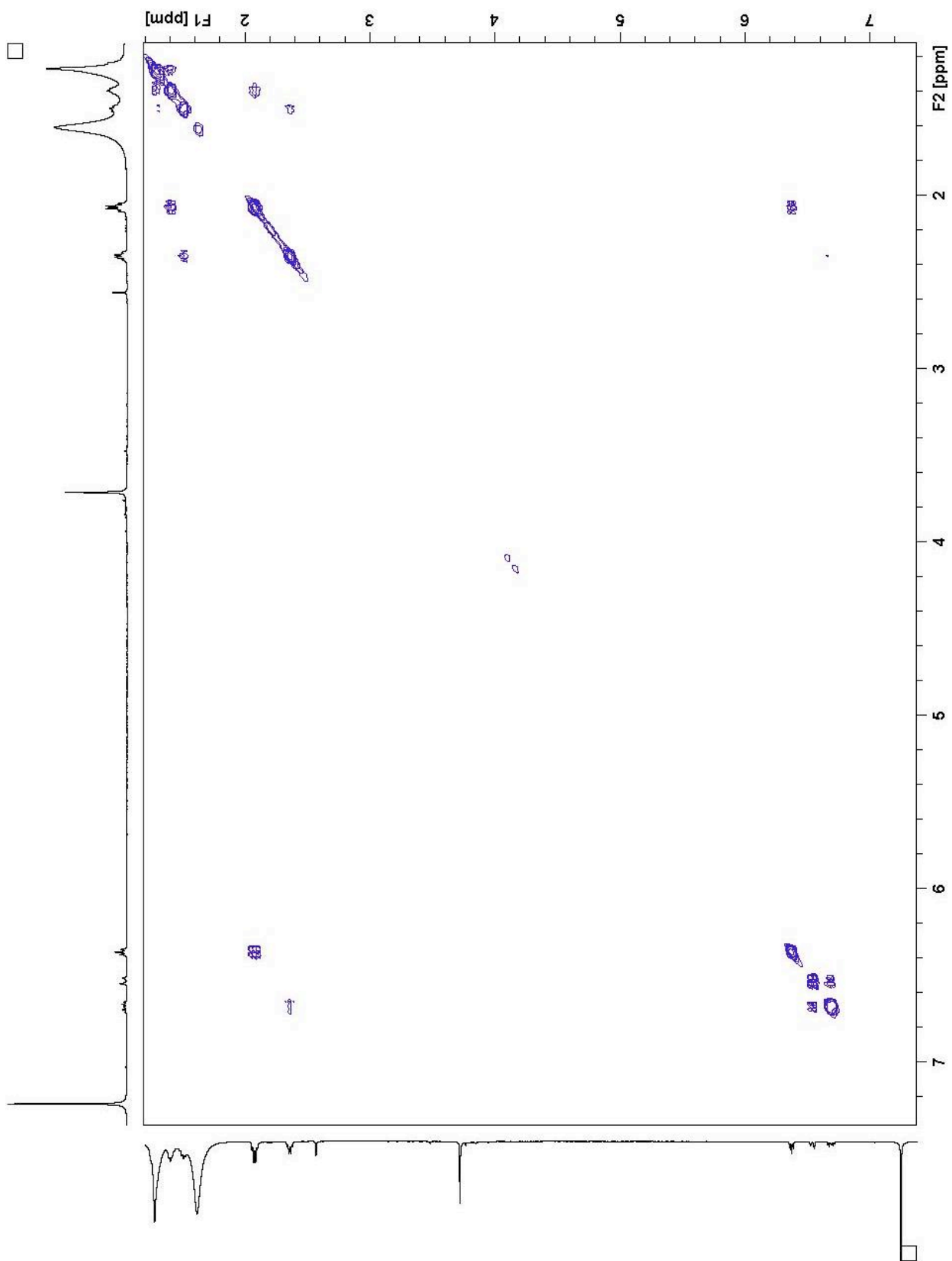


Figure S34. COSY spectrum of (4*E*)-*R*-antazarine (**7**) in CDCl₃.

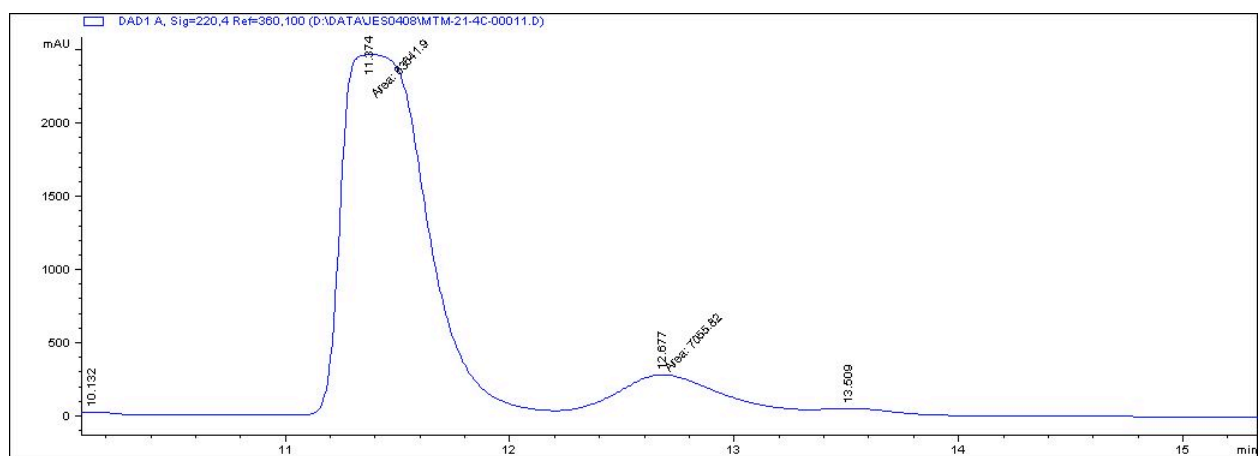


Figure S35. Chiral HPLC of motualevic acid F (**6**).